

Universal bifurcation patterns in the unfolding of a pair of homoclinic tangencies

Sergey Gonchenko¹, Dongchen Li², Dmitry Turaev²

¹Lobachevsky State University of Nizhny Novgorod, Scientific and Educational Mathematical Center “Mathematics of Future Technologies”, Nizhny Novgorod, Russia

²Department of Mathematics, Imperial College London

e-mail: sergey.gonchenko@mail.ru; d.li@imperial.ac.uk; d.turaev@imperial.ac.uk;

Abstract. We study generic two- and three-parameter unfoldings of a pair of orbits of quadratic homoclinic tangency in strongly dissipative systems. We prove that the corresponding stability windows for periodic orbits have various universal forms: the so-called “shrimps” (cross-road areas), as well as spring and saddle areas, and (in three-parameter unfoldings) “pregnant shrimps” – specific types of transitions between the shrimps and spring or saddle areas.

1 Introduction

Numerous studies of chaotic dynamics in models of vastly different physical nature reveal universal repetitive patterns in the bifurcation set in parameter space. These are the so-called “shrimps” [1, 2, 3, 4, 5], and also “squids” and “cockroaches” [6, 7, 8]. This phenomenon was discovered by C. Mira and coworkers in [9, 10, 11, 12] where less zoologically charged names were used – “cross-road area”, “saddle area”, and “spring area”, see Fig. 1. It is well-known that chaos in non-hyperbolic systems exhibits “stability windows” – regions in parameter space which correspond to emergence of stable periodic orbits. In the simplest case of strongly dissipative maps, the boundary of a stability window corresponds to a saddle-node bifurcation, where the stable periodic orbit is born, and to a period-doubling bifurcation, where the periodic orbit becomes unstable.¹ The curious phenomenon which we discuss in this paper is that quite often these two stability

¹We call a map strongly dissipative (or sectionally dissipative) if it contracts two-dimensional areas, so no orbit can have more than one positive Lyapunov exponent. If this is not the case, then another stability boundary can exist which corresponds to the birth of an invariant torus, leading to bifurcation patterns

boundaries do not simply go parallel to each other (forming "window streets" by the terminology of [5]) but somehow conspire to form non-trivial patterns mentioned above.

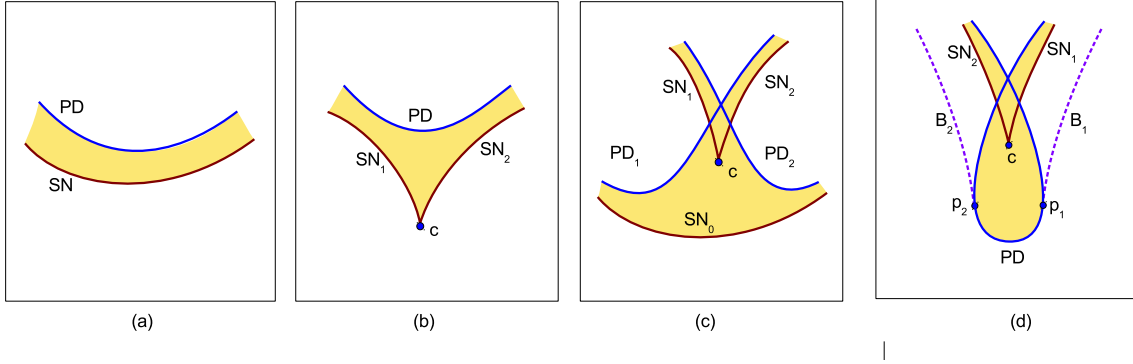


Figure 1: Examples of universal windows of stability: (a) "band-like area" called also "stability window street"; (b) "saddle area" – "squid"; (c) "cross-road area" – "shrimp"; (d) "spring area" – "cockroach". We denote by SN and PD curves of saddle-node (fold) and period-doubling (flip) bifurcations for fixed points and by B a fold curve for period-2 points. The points c and p correspond to codimension-2 bifurcations of fixed points – pitch-fork (cusp point c) and degenerate flip (with zero first Lyapunov value).

We explain this by the ubiquity of homoclinic tangencies. Chaotic dynamics are in general associated with hyperbolic sets and, in particular, to saddle periodic orbits and orbits of the intersection of their stable and unstable manifolds, the homoclinics. If we observe changes in the structure of chaos when parameters of the system change, it is natural to expect that the structure of the set of homoclinic orbits changes too, and non-transverse homoclinics appear at some parameter values, see Fig. 2. According to the Newhouse theorem [15, 16, 17, 18], this implies that parameter values corresponding to homoclinic tangencies are dense in some open regions in the parameter space. It is plausible that at least in the context of strongly dissipative maps these open regions cover all parameter values corresponding to non-hyperbolic chaotic dynamics [19, 21, 20, 22]. It was discovered by Gavrilov and Shilnikov [23] and Newhouse [24] that unfolding a homoclinic tangency in a strongly dissipative system is accompanied by the birth of stable periodic orbits. Thus, we can conclude that the particular stability windows that emerge due to bifurcations of homoclinic tangencies should be universally present in chaotic models of arbitrary nature.

A generic one-parameter unfolding of a quadratic homoclinic tangency creates simpler than those discussed in this paper, see e.g. [13]. Note also that in systems of differential equations (as opposed to maps) stability boundaries may also correspond to homoclinic loops or to a blue-sky catastrophe, even in the case of strong dissipation, see [14]. We leave all these situations aside.

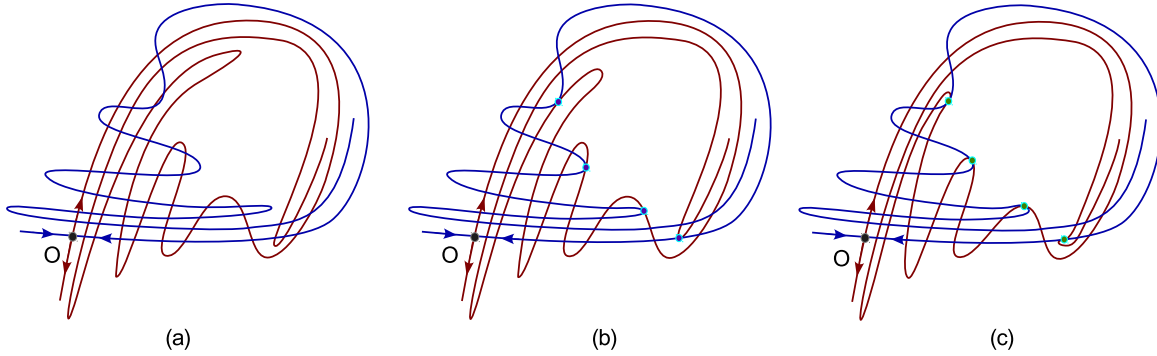


Figure 2: Homoclinic structures associated with a saddle fixed point O : (a) transverse homoclinics; (b) creation of a quadratic homoclinic tangency; (c) creation of a cubic homoclinic tangency (in general, two parameters are needed for this, see e.g. [21]).

ple stability windows (the so-called “window streets” or “band-like areas”) as in Fig. 1a. These are intervals of parameter values bounded by a saddle-node bifurcation and a period-doubling bifurcation, see [23, 25]. However, it was shown in [19, 21], that bifurcations of a homoclinic tangency can never be completely captured by any finite-parameter unfolding: increasing the number of independent parameters leads to new phenomena of a higher codimension, i.e., to phenomena that are not typically present in unfoldings governed by a smaller number of parameters. Thus, a two-parameter unfolding of a quadratic homoclinic tangency creates cubic homoclinic tangencies [21, 26]. The two-parameter stability windows near a cubic tangency were studied in [6] and they are exactly the “saddle area” (the “squid”) and the “spring area” (the “cockroach”) of Fig. 1(b) and (d). It is also shown in [21] that a two-parameter unfolding of a single quadratic homoclinic tangency creates a pair of homoclinic tangencies. In the current paper we study the stability windows due to the simultaneous breakup of two orbits of homoclinic tangency and show that they have a form of a “shrimp” (the “cross-road”) area.

We also study a generic three-parameter unfolding of a pair of orbits of quadratic homoclinic tangency and show that the corresponding stability windows in the three-dimensional parameter space have a form of “pregnant shrimps” – specific types of transitions between the cross-road, spring and saddle areas, as described in [10, 11, 12]. Thus, whenever we consider a model with chaotic behavior, in the Newhouse regions in two-dimensional or three-dimensional parameter space there must exist, in abundance, stability windows of these particular shapes.

2 Problem setting and results

2.1 Simplest periodic orbits near a double homoclinic tangency

Consider a C^r -smooth ($r \geq 2$) diffeomorphism f of an $(n+1)$ -dimensional ($n \geq 1$) smooth manifold. Let f have a saddle periodic point O with a one-dimensional unstable and an n -dimensional stable invariant manifolds $W^u(O)$ and $W^s(O)$. Assume that there exist two homoclinic orbits Γ_1 and Γ_2 such that $W^s(O)$ and $W^u(O)$ have *quadratic tangency* at the points of these two orbits (see Fig. 3(a)).

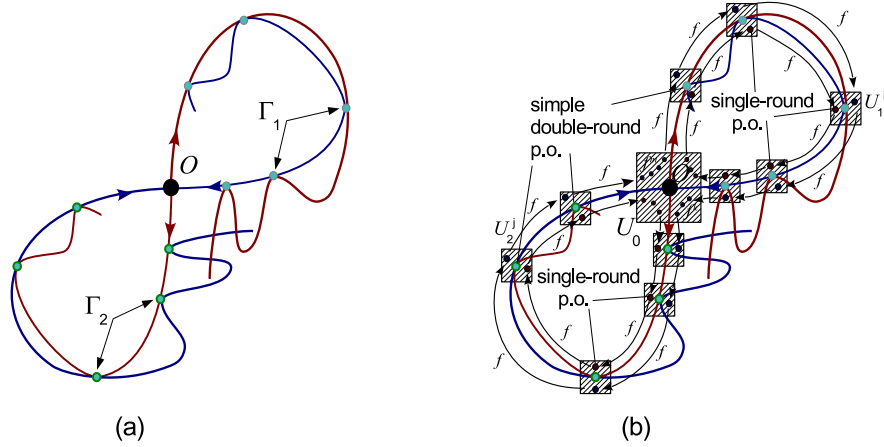


Figure 3: (a) A pair of homoclinic tangencies to a fixed point O of a two-dimensional diffeomorphism; (b) a neighborhood U of $O \cup \Gamma_1 \cup \Gamma_2$; here $U = U_0 \cup U_1 \cup U_2$, where U_0 is a small disc containing O , the handles $U_1 = \bigcup_{k=1}^{n_1} U_1^k$ and $U_2 = \bigcup_{k=1}^{n_2} U_2^k$ consist of small neighborhoods of those points of the orbits Γ_1 and Γ_2 that do not belong to U_0 . The iterations of f for single-round and simple double-round periodic orbits are also shown schematically.

The closure of the homoclinic orbits $\Gamma_{1,2}$ is the union of $\Gamma_{1,2}$ and the orbit $L = \{f^j(O)\}_{j=0}^{\tau-1}$ of the point O (where τ is a period of O , i.e., $f^\tau(O) = O$). We take a small neighborhood U of the set of these three orbits. Our goal is to study bifurcations of simplest periodic orbits lying in U .

Let U_0 be a small ball around O . Since the orbit Γ_i ($i = 1, 2$) is homoclinic, only finitely many points in Γ_i lie outside of the neighborhood $\tilde{U}_0 = \bigcup_{j=0}^{\tau-1} f^j(U_0)$ of L . Namely, on Γ_i there are points $P_i^+ \in W_{loc}^s(O) \cap U_0$ and $P_i^- \in W_{loc}^u(O) \cap U_0$ such that $P_i^+ = f^{N_i} P_i^-$ for some $N_i > 0$ while $f^j(P_i^-) \notin \tilde{U}_0$ for $j = 1, \dots, N_i - 1$.

Note that U is a disjoint union of \tilde{U}_0 and a small neighborhoods U_1 and U_2 of $\Gamma_1 \setminus \tilde{U}_0$

and, respectively, $\Gamma_2 \setminus \tilde{U}_0$ (the set U_i is a disjoint union of small balls around the points $f^j P_i^-$, $j = 1, \dots, p_i - 1$, see Fig. 3(b)). As L is hyperbolic, no other orbit can lie entirely in \tilde{U}_0 . So, any periodic orbit in U , other than L , must visit $U_1 \cup U_2$. The same is true for any map which is C^1 -close to f : there is a uniquely defined hyperbolic continuation of L in \tilde{U}_0 and any other orbit in U must visit $U_1 \cup U_2$.

A periodic orbit in U is called *single-round* if it visits only U_1 or only U_2 , and does it exactly once. A *simple double-round* periodic orbit visits U_1 , gets into \tilde{U}_0 , then leaves it and goes to U_2 , and finally returns to \tilde{U}_0 and closes up.

Single-round orbits stay in a small neighborhood of only one of the orbits of homoclinic tangency, Γ_1 or Γ_2 , so their bifurcations are described by the theory of a homoclinic tangency, which starts with the work of Gavrilov and Shilnikov [23], see [25, 27, 28] for the multidimensional case. We, therefore, focus in this paper on the new case – the simple double-round periodic orbits.

We call the map $T_0 = f^\tau|_{U_0}$ the *local map* near the point O . We will also consider the *global maps* T_1 and T_2 , where T_i is the restriction of f^{N_i} onto a sufficiently small ball around P_i^- , so it acts from a small neighborhood of P_i^- to a small neighborhood of P_i^+ . The maps T_0 and $T_{1,2}$ remain well-defined for any C^1 -small perturbation of f .

By definition, a single-round orbit corresponds to a fixed point of the first-return map $T_i T_0^k$ for some sufficiently large integer k and $i = 1$ or $i = 2$. The simple double-round orbits are defined as those corresponding to fixed points of the first-return map $T_{km} = T_2 T_0^m T_1 T_0^k$ for some sufficiently large integers m and k . We will call them (k, m) -orbits.

A very similar construction is applicable for dynamical systems with continuous time. Namely, we consider in this case a C^r -smooth ($r \geq 2$) system of differential equations or, equivalently, a C^r -smooth vector field f on an $(n + 2)$ -dimensional ($n \geq 1$) smooth manifold. Let f have a saddle periodic orbit L , and let O be a point of intersection of this periodic orbit with a small $(n + 1)$ -dimensional cross-section U_0 . Let \tilde{U}_0 be a sufficiently small neighborhood of L . Then, the *local map* T_0 is defined as the map of first return to U_0 by the orbits of the flow defined by f , which lie in the neighborhood \tilde{U}_0 .

We assume that the unstable manifold $W^u(O)$ is one-dimensional and the stable manifold $W^s(O)$ is n -dimensional and that $W^u(O)$ and $W^s(O)$ have two orbits of quadratic homoclinic tangency, Γ_1 and Γ_2 . On Γ_i , we take points $P_i^+ \in W_{loc}^s(O) \cap U_0$ and $P_i^- \in W_{loc}^u(O) \cap U_0$, and denote as U_i a small neighborhood of the segment of Γ_i between the points P_i^- and P_i^+ . The *global maps* T_i ($i = 1, 2$) are defined as maps from a sufficiently small ball around P_i^- in U_0 to a small ball around P_i^+ in U_0 along the orbits lying in U_i .

These maps remain well-defined for any C^1 -small perturbation of f .

A periodic orbit in $U = \tilde{U}_0 \cup U_1 \cup U_2$ is *single-round* if it visits only U_1 or only U_2 , and does it exactly once. A *simple double-round* periodic orbit visits U_1 , gets into \tilde{U}_0 , then leaves it and goes to U_2 , and finally returns to \tilde{U}_0 and closes up. By definition, a single-round orbit corresponds to a fixed point of the first-return map $T_i T_0^k$ in a small neighborhood of P_i^+ in U_0 for some sufficiently large integer k and $i = 1$ or $i = 2$. The simple double-round orbits (k, m) -orbits are defined as those corresponding to fixed points of the first-return map $T_{km} = T_2 T_0^m T_1 T_0^k$ in a small neighborhood of P_i^+ in U_0 for some sufficiently large integers m and k .

All the arguments in the proofs of the results below are done in terms of the local and global maps only and, with the above notations, are identical for the cases of discrete and continuous time (i.e., diffeomorphisms and smooth flows). We therefore adopt a neutral terminology in the formulation of the results, simply calling f a *dynamical system*, implying that all the theorems hold true in both cases.

2.2 Two-parameter unfoldings

We start with analyzing bifurcations of the (k, m) -orbits in a generic two-parameter unfolding of the homoclinic tangencies of f . Consider a two-parameter family f_ε , which depends smoothly on $\varepsilon = (\varepsilon_1, \varepsilon_2)$, and let f_0 be the original system f . Introduce coordinates $(x, y) \in \mathbb{R}^n \times \mathbb{R}$ in U_0 such that the local stable and unstable manifolds are given for all small ε by the equations $y = 0$ and $x = 0$, respectively. Define the *splitting parameter* μ_i for the tangency Γ_i as the y -coordinate of the point $T_i P_i^-$ (see Lemma 3). The splitting parameters are smooth functions of ε . The pair of tangencies is said to *unfold generically* if

$$\det \frac{\partial(\mu_1, \mu_2)}{\partial(\varepsilon_1, \varepsilon_2)} \neq 0. \quad (1)$$

This will be our standing assumption; it allows us to take $\mu = (\mu_1, \mu_2)$ as new parameters, so we will use the notation f_μ from now on.

Denote by $\lambda_1, \dots, \lambda_n, \gamma$ the multipliers of O (the eigenvalues of the derivative matrix of T_0 at O) ordered such that

$$|\gamma| > 1 > |\lambda_1| \geq \dots \geq |\lambda_n|.$$

Our main assumption on f is the *strong dissipativity* (also called sectional dissipativity) condition

$$|\lambda_1 \gamma| < 1. \quad (2)$$

In general, bifurcations of single-round orbits near a homoclinic tangency can be quite complicated [28]. In the strongly dissipative case, however, the situation is simpler. It immediately follows from [23, 25] that in the (μ_1, μ_2) -parameter plane there are infinitely many bands (“stability window streets”) σ_k^1 and σ_k^2 accumulating at the axes $\mu_1 = 0$ and $\mu_2 = 0$, respectively, as $k \rightarrow \infty$. The bands σ_i^α and σ_j^α , where $\alpha = 1, 2$, do not intersect if $i \neq j$. The boundaries of σ_k^α and σ_k^α are curves corresponding to nondegenerate saddle-node (SN) and period-doubling (PD) bifurcations for orbits of period k , see Fig. 4.

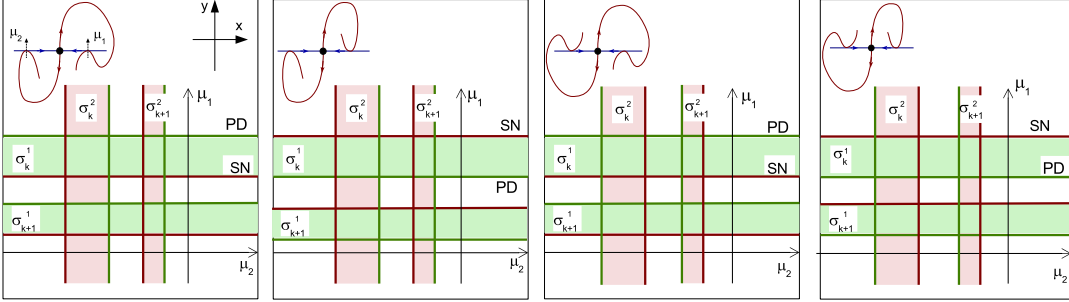


Figure 4: Bands σ_k^1 and σ_k^2 in the (μ_1, μ_2) -parameter plane for various types of double homoclinic tangencies in the case $\gamma > 0$. Here we assume that the homoclinic Γ_i split in such a way that $T_i W_{loc}^u(O)$ and $W_{loc}^s(O)$ do not intersect near P_i^+ for $\mu_i < 0$ and intersect at two points at $\mu_i > 0$. Horizontal (green) and vertical (pink) bands correspond to stability window streets for single-round periodic orbits that lie, respectively, in U_1 and in U_2 .

The structure of stability windows for simple double-round orbits is different, as follows from Theorem 1 below. Denote

$$\theta = -\frac{\ln |\lambda_1|}{\ln |\gamma|}. \quad (3)$$

Note that the strong dissipativity condition (2) implies $\theta > 1$.

Theorem 1. *Take any $\delta > 0$. If $\theta > 1$, and the two homoclinic tangencies are quadratic, then for every sufficiently large integers m and k satisfying*

$$(\theta + \delta)^{-1} < \frac{m}{k} < \theta - \delta, \quad (4)$$

there is a disc $\Delta_{k,m}$ in the (μ_1, μ_2) -plane and a ball $B_{k,m} \subset U_0$ such that the return map T_{km} is defined on $B_{k,m}$ for $\mu \in \Delta_{k,m}$ and, after an affine change of coordinates and parameters $R_{k,m} : (x, y, \mu_1, \mu_2) \mapsto (X, Y, M_1, M_2)$, takes the form $T_{km}|_{B_{k,m}} : (X, Y) \mapsto (\bar{X}, \bar{Y})$, where

$$\begin{aligned} \bar{X} &= o_r(1)_{k,m \rightarrow +\infty}, \\ \bar{Y} &= M_2 - (M_1 - Y^2)^2 + o_r(1)_{k,m \rightarrow +\infty}. \end{aligned} \quad (5)$$

Here $o_r(1)_{k,m \rightarrow +\infty}$ stands for terms tending to zero along with all derivatives up to order r as $k, m \rightarrow +\infty$. As $k, m \rightarrow +\infty$, the discs Δ_{km} converge to the origin $(\mu_1, \mu_2) = 0$ and the balls B_{km} converge to the homoclinic point P_2^+ (see Fig. 5a). The image of $B_{km} \times \Delta_{km}$ by the rescaling map R_{km} covers a centered at zero ball whose radius grows to infinity as the integers k, m satisfying condition (4) tend to $+\infty$.

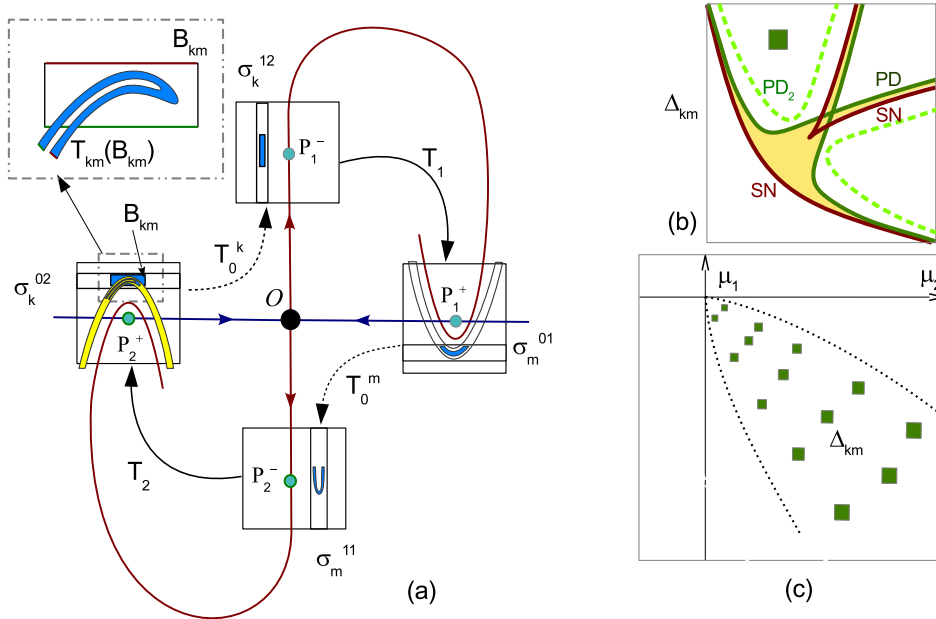


Figure 5: (a) The first-return map T_{km} for simple double-round (k, m) -orbits; (b) the shrimp-like structure of a bifurcation set in Δ_{km} ; (c) a cascade of the shrimp-like stability windows in the case of a double homoclinic configuration of Fig.(a).

This result (see the proof in Section 4) implies that bifurcations of the (k, m) -orbits for large (k, m) satisfying condition (4) are the same as bifurcations of the fixed points of the one-dimensional map ²

$$\bar{Y} = M_2 - (M_1 - Y^2)^2. \quad (6)$$

Its bifurcations are well studied [9, 10, 11, 12]; the bifurcation curves corresponding to the saddle-node and period-doubling bifurcations of the fixed points form the “shrimp” (the “cross-road area”) pattern as in Fig. 5b. Thus, Theorem 1 shows that

- in generic two-parameter families of strongly dissipative systems, points corresponding to the existence of a pair of homoclinic tangencies are accumulated by a cascade of the shrimp-like stability windows, see Fig. 5c.

²Strictly speaking, it is true when $r \geq 5$ - because the map (6) can undergo the codimension-2 flip (period-doubling) bifurcation where the first Lyapunov value vanishes and the second one is non-zero (the calculation of the second Lyapunov value requires at least five derivatives).

Of course, one does not need to be restricted by bifurcations of fixed points only: by Theorem 1, whichever non-degenerate bifurcations of codimension 1 and 2 are present in map (6), they are repeated infinitely many times in any generic two-parameter unfolding of a pair of homoclinic tangencies of a strongly dissipative system.

The idea of rescaling the first-return map was first proposed in [29] for the study of a single quadratic homoclinic tangency. For a single n -th order homoclinic tangency, the first-return map in a generic $(n-1)$ -parameter unfolding gets, after a rescaling, arbitrarily close to the polynomial map

$$\bar{Y} = \sum_{i=0}^{n-2} M_{i+1} Y^i \pm Y^n,$$

where we can always take the minus sign in front of Y^n when n is even, see [30, 31]. For $n = 2$ (quadratic tangency), this gives us the parabola map

$$\bar{Y} = M_1 - Y^2;$$

a cubic homoclinic tangency gives rise to the maps

$$\bar{Y} = M_1 + M_2 Y \pm Y^3.$$

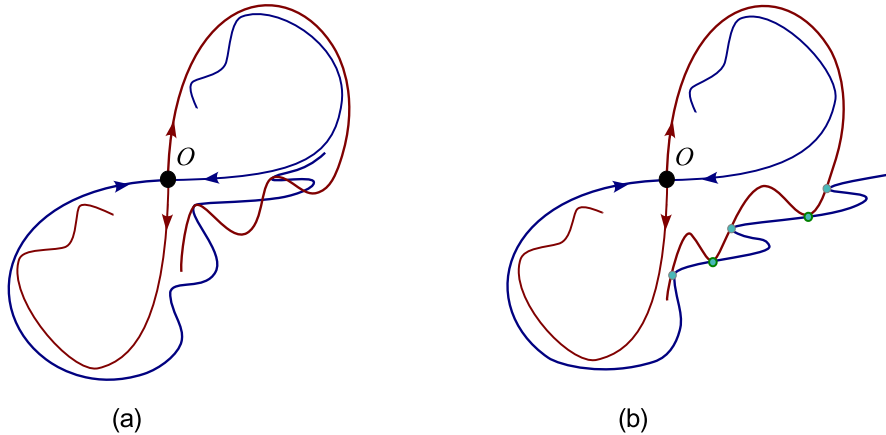


Figure 6: A schematic picture at perturbations of a diffeomorphism from Fig. 3(a) of (a) a double-round cubic homoclinic tangency and (b) a pair of double-round homoclinic tangencies.

The stability windows for the parabola map and the cubic maps are shown in Figure 1: the “window streets” appear in the parabola map; the so-called “saddle area” (“squid”) and the “spring area” (“cockroach”) patterns appear in the cubic maps with, respectively, the “+” and “-” sign [6, 30]. Along with the shrimp pattern produced by the double

parabola map (6), they form the 4 universal bifurcation patterns that appear in generic two-parameter families of strongly dissipative systems from the Newhouse domain. In particular, one can show (cf. [21, 32]) that the splitting of two quadratic homoclinic tangencies creates points in the (μ_1, μ_2) -plane that correspond to a cubic tangency, see Fig. 6b. So all the 4 patterns are present in a generic two-parameter family f_μ which we consider here. For example, we see these patterns in the parameter plane of a periodically perturbed autonomous system with a homoclinic figure-eight. Thus, in [33] the existence of infinite cascades of parameter values corresponding to cubic and pairs of quadratic homoclinic tangencies was proven, and cascades of stability windows of different types were found, see Fig. 7.

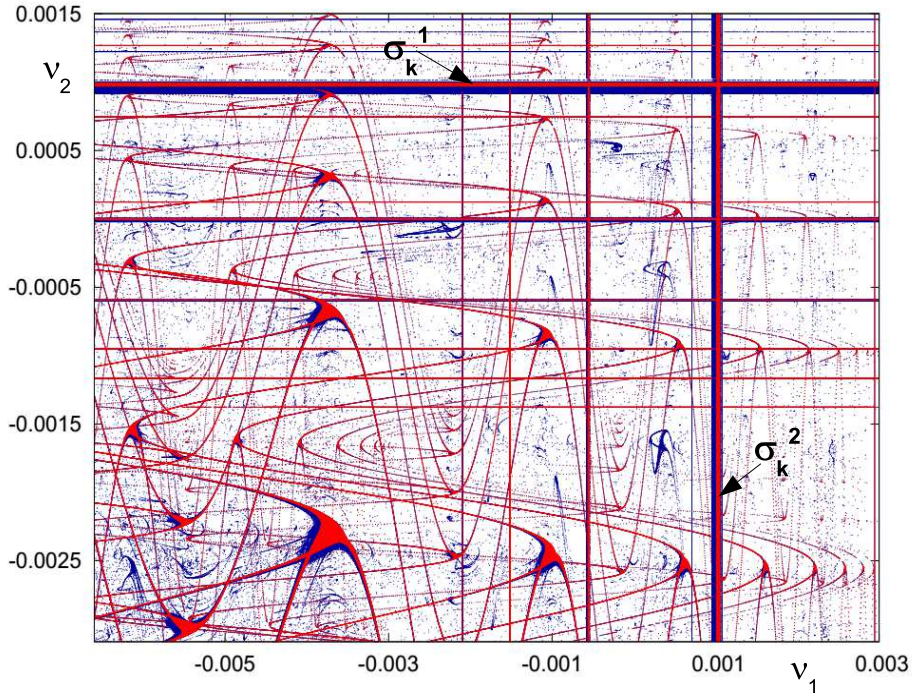


Figure 7: Bifurcation sets in the (ν_1, ν_2) -parameter plane for a periodically perturbed system with a homoclinic figure-eight; red stability windows correspond to single-round periodic orbits and blue windows to multi-round periodic orbits).

2.3 Three-parameter unfoldings and the main theorem

By itself, the result of Theorem 1 is not surprising: as a single round near a homoclinic tangency scales to the parabola map, it is natural that passing along two homoclinic tangencies gives rise to the composition of the parabola maps. A similar result can be

extracted e.g. from [34]. However, we want to stress that bifurcations of (k, m) -orbits are, in fact, richer than what happens in map (6). Our main result, Theorem 2, shows that the bifurcation patterns for the (k, m) -orbits which violate condition (4) are generated by the three-parameter family of maps

$$\bar{Y} = M_2 - (M_1 - Y^2)^2 + M_3 Y. \quad (7)$$

Accordingly, the description of the stability windows for such orbits requires the analysis of a *three-parameter unfolding* of the map f . The choice of the third control parameter depends on whether the point O is a saddle or a saddle-focus. We assume that λ_1 , the largest (in the absolute value) of the multipliers inside the unit circle, is simple. It is either real or complex; in the latter case $\lambda_1 = \lambda_2^*$. We assume that

$$|\gamma| > 1 > |\lambda_1| > |\lambda_j| \quad \text{for } j > 1$$

if λ_1 is real – then O is called a *saddle*, or

$$|\gamma| > 1 > \lambda > |\lambda_j| \quad \text{for } j > 2$$

if $\lambda_{1,2} = \lambda e^{\pm i\varphi}$ where $\varphi \in (0, \pi)$ – then O is called a *saddle-focus*.

We consider C^r -families of systems (diffeomorphisms or flows) f_ε , $\varepsilon = (\varepsilon_1, \varepsilon_2, \varepsilon_3)$, where f_0 is the original system f with a pair of orbits of homoclinic tangency. The splitting parameters $\mu_{1,2}$, the ratio θ defined by (3) and the argument φ of λ_1 (when λ_1 is complex) are smooth functions of ε . We put $\mu_3 = \theta(\varepsilon) - \theta(0)$ if O is a saddle, and $\mu_3 = \varphi(\varepsilon) - \varphi(0)$ if O is a saddle-focus. Assume that

$$\det \frac{\partial(\mu_1, \mu_2, \mu_3)}{\partial(\varepsilon_1, \varepsilon_2, \varepsilon_3)} \neq 0, \quad (8)$$

which allows us to write the family as f_μ with $\mu = (\mu_1, \mu_2, \mu_3)$.

Recall that θ and φ are continuous invariants (moduli) of topological equivalence of systems with homoclinic tangencies: if two systems have different values of θ or φ , they are not topologically equivalent [35, 36, 37]. In some cases they are also moduli of the Ω -equivalence (topological equivalence on the set of nonwandering orbits) [38, 30, 39, 40]. This means that any change in the values of θ or φ leads to bifurcations of non-wandering orbits, e.g. periodic orbits, even when the tangency is not split [41, 35, 32]. Therefore, using the moduli as control parameters is natural in the study of homoclinic bifurcations [42, 21, 27, 43, 30, 44, 26, 28].

The last assumption we need for Theorem 2, is that both homoclinic tangencies Γ_1 and Γ_2 are *simple*. The simplicity condition is a version of the quasi-transversality condition from [45]. For two-dimensional maps with a saddle and three-dimensional maps with

a saddle-focus, every quadratic homoclinic tangency is automatically simple. In higher dimensions, the stable manifold $W_{loc}^s(O)$ contains the strong stable invariant submanifold $W_{loc}^{ss}(O)$. This submanifold is C^r -smooth and is uniquely defined by the condition that it is an invariant manifold tangent at O to the eigenspace (of the linearization of T_0 at O) corresponding to the multipliers $\lambda_2, \dots, \lambda_n$ in the case of saddle, and $\lambda_3, \dots, \lambda_n$ in the case of saddle-focus. We denote $n_s = 1$ if O is a saddle, and $n_s = 2$ if O is a saddle-focus. Then the strong-stable manifold is $(n - n_s)$ -dimensional. It is also well-known (see e.g. [14]) that W_{loc}^s carries a uniquely defined C^r -smooth strong-stable invariant foliation \mathcal{F}^{ss} consisting of $(n - n_s)$ -dimensional leaves; and W_{loc}^{ss} is the leaf of \mathcal{F}^{ss} which contains O . Another fact we use (see, for example, [46, 45, 47, 14]) is that the invariant unstable manifold $W^u(O)$ is a part of the extended unstable manifold W^{ue} which is an $(n_s + 1)$ -dimensional invariant manifold, tangent at O to the eigenspace corresponding to the eigenvalues γ and λ_1 if O is a saddle, or γ and λ_1, λ_2 , if O is a saddle-focus. The manifold W^{ue} is at least $C^{1+\epsilon}$. It is not uniquely defined, but it always contains W_{loc}^u and any two such manifolds are tangent to each other at the points of W_{loc}^u (see Fig. 8).

We can now interpret the simplicity condition as

- (C1) The homoclinic orbits Γ_i ($i = 1, 2$) do not have points in the strong-stable manifold (i.e., $M_i^+ \notin W_{loc}^{ss}(O)$).
- (C2) The extended unstable manifold is transverse to the strong-stable foliation at the points of Γ_1 and Γ_2 , that is, $T_i W_{loc}^{ue}$ is transverse at the point P_i^+ to the leaf of \mathcal{F}^{ss} which passes through this point. (See Fig. 8 for an illustration).

Theorem 2. *If the system is strongly dissipative and the two tangencies are quadratic and simple (i.e., C1 and C2 are satisfied), then there exists a sequence of integers $k, m \rightarrow +\infty$ such that for every sufficiently large k and m from this sequence, there exists a region Δ_{km} in the (μ_1, μ_2, μ_3) -space and a ball $B_{km} \subset U_0$ such that after a change of coordinates and parameters $R_{km} : (x, y, \mu_1, \mu_2, \mu_3) \mapsto (X, Y, M_1, M_2, M_3)$, which is a composition of a transformation independent of k and m and an affine transformation with k, m -dependent coefficients, the return map T_{km} on B_{km} for $\mu \in \Delta_{km}$ takes the form $T_{km}|_{B_{km}} : (X, Y) \mapsto (\bar{X}, \bar{Y})$:*

$$\begin{aligned}\bar{X}_1 &= M_1 - Y^2 + o_r(1)_{k,m \rightarrow +\infty}, \\ \bar{X}_2 &= o_r(1)_{k,m \rightarrow +\infty}, \\ \bar{Y} &= M_2 - (M_1 - Y^2)^2 + M_3 Y + o_r(1)_{k,m \rightarrow +\infty}.\end{aligned}\tag{9}$$

As $k, m \rightarrow +\infty$, the balls Δ_{km} converge to the origin $\mu = 0$ and the balls B_{km} converge to the homoclinic point P_1^+ . If O is a saddle-focus, the image of $B_{km} \times \Delta_{km}$ by the rescaling R_{km} covers a centered at zero ball whose radius grows to infinity as $k, m \rightarrow +\infty$. If O is a saddle, then the image of $B_{km} \times \Delta_{km}$ by R_{km} covers the intersection of a centered at zero ball whose radius grows to infinity as $k, m \rightarrow +\infty$ and either the set $M_3 > \delta_{km}$ or the set $M_3 < -\delta_{km}$ where δ_{km} is a converging to zero sequence of positive numbers.

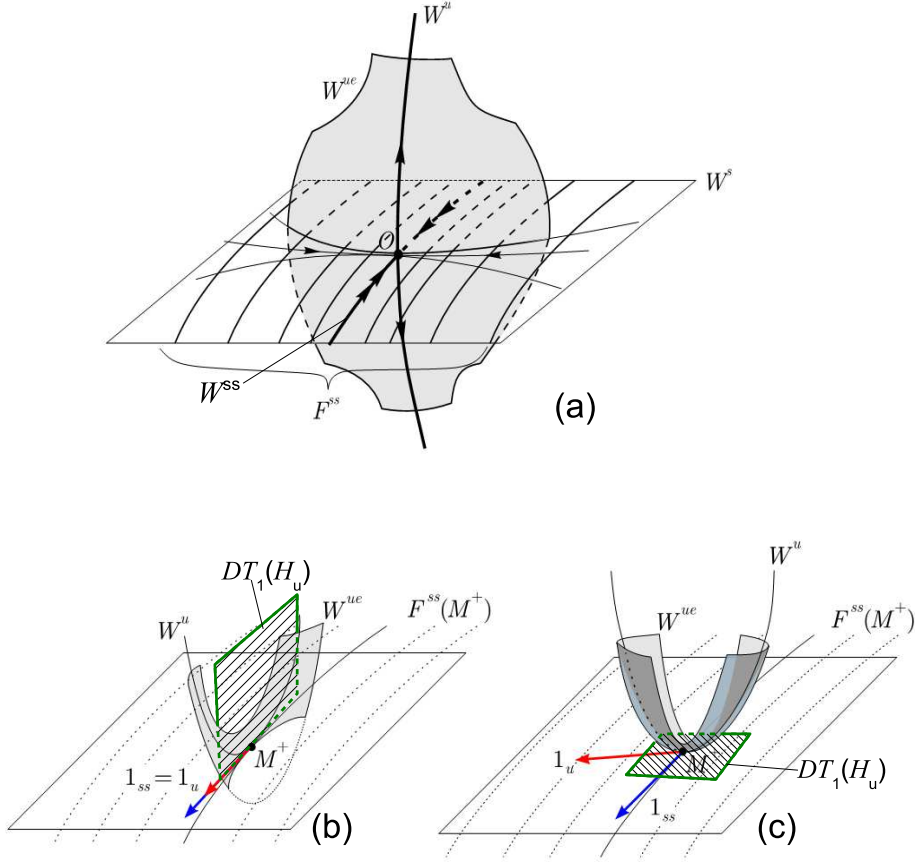


Figure 8: (a) A geometric illustration of the invariant manifolds (W^u , W^s , W^{ss} , W^{ue}) and foliation \mathcal{F}^{ss} existing near the fixed point O ; (b) and (c) are examples of two types of non-simple homoclinic tangencies which correspond two different cases of nontransversality of W^{ue} and $\mathcal{F}^{ss}(P^+)$.

The proof is given in Section 4, along with the formulas for the transformation R_{km} that relates the original coordinates and parameters and the rescaled ones. Note that non-zero finite values of M_3 correspond, in the case of saddle, to $\lambda_1^k \gamma^m$ (if $m > k$) or $\lambda_1^m \gamma^k$ (if $m < k$) being bounded away from zero and infinity. This implies $m/k \rightarrow \theta$ or, respectively, $k/m \rightarrow \theta$ as $k, m \rightarrow +\infty$, so Theorem 2 gives, in the saddle case, the first-return map for orbits corresponding to the (k, m) values at the border of those described by Theorem 1 (see condition (4)). In the saddle-focus case there are no restrictions on m/k , as the parameter M_3 strongly depends on φ . Note also that in the saddle case M_3 has a definite sign for a given (k, m) ; it can be different for another pair (k, m) , depending

on the sign of λ_1 and γ and the coefficients of the global maps $T_{1,2}$, see the proof of Theorem 2 for details.

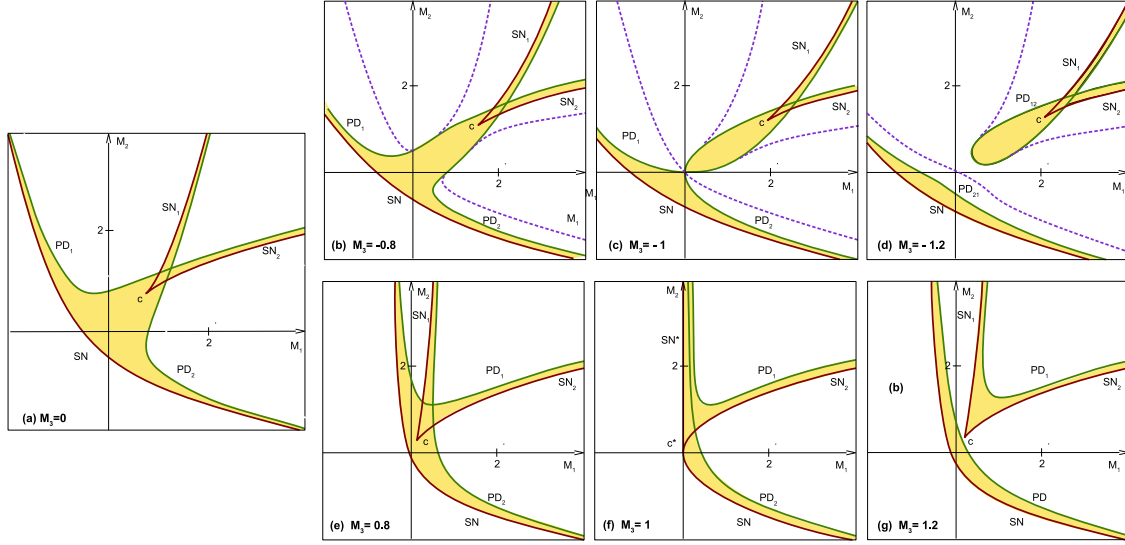


Figure 9: An example of transition, in map (7), from a “shrimp” to a “cockroach” when $M_3 < 0$, based on [10]; and from “shrimp” to “squid” when $M_3 > 0$, based on [12]. Here we show bifurcation curves for fixed points, saddle-node (SN) and period-doubling (PD) ones, as well as the saddle-node bifurcation curves (dashed lines) for period-2 points. (a) “Shrimp” in the (M_1, M_2) -plane; (b) “pregnant shrimp”; (c) the point $(M_1 = 0, M_2 = 0)$ corresponds to a codimension-3 bifurcation, when the fixed point $Y = 0$ has the multiplier -1 and zero first and second Lyapunov values (the map becomes $\bar{Y} = Y - Y^4$); (d) “cockroach”; (e) “shrimp”; (f) the point $(M_1 = 0, M_2 = 0)$ corresponds to a codimension-3 bifurcation, when the fixed point $Y = 0$ has the multiplier 1 and zero first and second Lyapunov values (the map becomes $\bar{Y} = -Y - Y^4$); (g) “squid”: the curves SN and PD_2 are separated.

By Theorem 2, the generic three-parameter unfolding of the pair of simple quadratic homoclinic tangencies exhibits a cascade of stability windows whose shape is the same as in the three-parameter family (7) (possibly restricted to only positive or negative values of M_3). This family was studied e.g in [10, 12]. The change in the structure of the stability windows in the (M_1, M_2) -parameter plane when M_3 varies is shown in Fig. 9. Note that the cases $M_3 < 0$ and $M_3 > 0$ are different. When $M_3 < 0$, one can see the transition from a “shrimp” to a “pregnant shrimp” to a “cockroach”; when $M_3 > 0$, the “shrimp” - “squid” transition happens. A detailed analysis of these and other transitions was done in [10, 11, 12, 48].

3 Normal forms of the local and global maps

Let f_ε be a generic unfolding family of C^r diffeomorphisms ($r \geq 2$), where $f_0 = f$ is strongly dissipative and has a pair of orbits of quadratic homoclinic tangency. As mentioned before, we will consider for Theorem 1 the two-parameter unfolding with $\mu = (\mu_1, \mu_2)$ consisting of two splitting parameters, and for Theorem 2 the three-parameter unfolding with an additional parameter $\mu_3 = \theta(\varepsilon) - \theta(0)$ if O is a saddle, and $\mu_3 = \varphi(\varepsilon) - \varphi(0)$ if O is a saddle-focus. Due to conditions (1) and (8), we can just denote the family by f_μ .

Recall that the local map is defined as $T_0 \equiv f^r : U_0 \rightarrow U_0$, where U_0 is a small neighborhood of O ; we take points $P_i^+ \in W_{loc}^s(O) \cap \Gamma_i$ and $P_i^- \in W_{loc}^u(O) \cap \Gamma_i$ inside U_0 such that $P_i^+ = f^{N_i} P_i^-$ for some $N_i > 0$ while $f^j(P_i^-) \notin \tilde{U}_0$ for $j = 1, \dots, N_i - 1$. Now fix in U_0 some small neighborhoods $\Pi_i^+ \ni P_i^+$ and $\Pi_i^- \ni P_i^-$ satisfying $T_0(\Pi_i^+) \cap \Pi_i^+ = \emptyset$ and $T_0^{-1}(\Pi_i^-) \cap \Pi_i^- = \emptyset$. The global maps are $T_1 \equiv f^{N_1} : \Pi_1^- \rightarrow \Pi_1^+$ and $T_2 \equiv f^{N_2} : \Pi_2^- \rightarrow \Pi_2^+$, which are diffeomorphisms into their ranges.

Observe that the iterates $T_0^k(\Pi_i^+)$ intersect Π_j^- ($i, j = 1, 2$) for every sufficiently large k . The domain of $T_0^k : \Pi_i^+ \rightarrow \Pi_j^-$ consist of infinitely many pairwise disjoint strips $\sigma_k^{0ij} \subset \Pi_i^+$ which accumulate on $W_{loc}^s(O) \cap \Pi_i^+$ as $k \rightarrow +\infty$. Its range is formed by infinitely many strips $\sigma_k^{1ij} = T_0^k(\sigma_k^{0ij}) \subset \Pi_j^-$ accumulating on $W_{loc}^u(O) \cap \Pi_j^-$ as $k \rightarrow +\infty$ (see Fig. 10).

For the family f_ε , one can always consider such C^r -coordinates in U_0 that the fixed point O_ε of the local map T_0 is at the origin for all small ε , and hence we drop the subscription of O . Moreover, we can write $T_0(\varepsilon)$ in the form

$$\bar{x} = A_1 x + \dots, \quad \bar{u} = A_2 u + \dots, \quad \bar{y} = \gamma y + \dots, \quad (10)$$

where $x \in \mathbb{R}^{n_s}, y \in \mathbb{R}^1, u \in \mathbb{R}^{m-n_s}$, the dots stand for nonlinear terms, and the eigenvalues of the matrices A_1 and A_2 are the stable leading multipliers and the stable non-leading multipliers, respectively. We say that x are the leading (stable) coordinates and u are the non-leading ones. Note that if λ_1 is real, then $A_1 = \lambda_1$ and x is a scalar; and if λ_1 is complex, then $\lambda_1 = \bar{\lambda}_2 = \lambda e^{\pm i\varphi}$, $x = (x_1, x_2)$ and $A_1 = \lambda \begin{pmatrix} \cos \varphi & -\sin \varphi \\ \sin \varphi & \cos \varphi \end{pmatrix}$.

It is well-known that there is a C^r coordinate transformation straightening the local stable and unstable manifolds of O so that they acquire equations $W_{loc}^s = \{y = 0\}$ and $W_{loc}^u = \{x = 0, u = 0\}$ and the map T_0 takes, locally, the form

$$\begin{aligned} \bar{x} &= A_1(\varepsilon)x + g_1(x, u, y, \varepsilon), & \bar{u} &= A_2(\varepsilon)u + g_2(x, u, y, \varepsilon), \\ \bar{y} &= \gamma(\varepsilon)y + h(x, u, y, \varepsilon), \end{aligned} \quad (11)$$

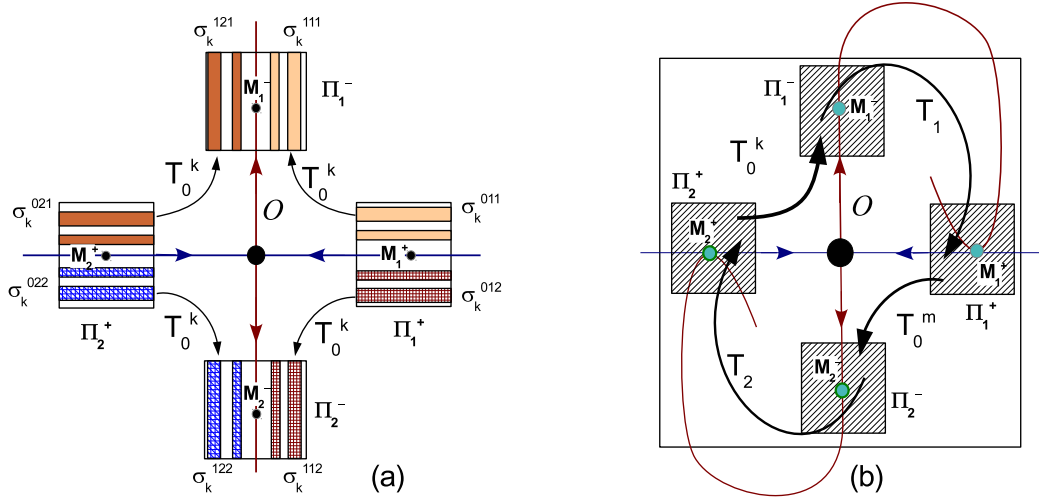


Figure 10: (a) The action of iterations of T_0 from $\sigma^{0ij} \in \Pi_i^+$ to $\sigma^{1ij} \in \Pi_j^-$. (b) A geometric structure of the homoclinic points M_1^+, M_1^-, M_2^+ and M_2^- and their neighborhoods. Schematic actions of the first return maps $T_{km} = T_2 \circ T_0^m \circ T_1 \circ T_0^k$.

where the nonlinearities $g_{1,2}$ and h vanish at the origin along with their first derivatives, and, moreover,

$$g(0, 0, y, \varepsilon) \equiv 0, \quad h(x, u, 0, \varepsilon) \equiv 0 \quad (12)$$

for (x, u, y, ε) small.

Bringing the local map to the form (11) is not enough for our purposes because, for a general choice of the functions g and h , the iterations T_0^k can deviate too much from its linear part. Essentially, this means that the right-hand side of (11) contains “too many” non-resonant terms. Fortunately, infinitely many of nonresonant terms can be eliminated by means of some additional smooth transformation of coordinates, as the following lemma from [28] shows. This lemma is a generalization of similar results of [49, 38, 37, 14] and allows us to achieve a higher (i.e., C^r) smoothness of the coordinate transformation.

Lemma 1. [28] *At all sufficiently small ε , there exists a local C^r -transformation of coordinates after which the map $T_0(\varepsilon)$ keeps its form (11),(12) while the functions p and q satisfy additional identities*

$$g_1(x, u, 0, \varepsilon) \equiv 0, \quad h(0, 0, y, \varepsilon) \equiv 0, \quad (13)$$

$$\frac{\partial g}{\partial x}(0, 0, y, \varepsilon) \equiv 0, \quad \frac{\partial h}{\partial y}(x, u, 0, \varepsilon) \equiv 0. \quad (14)$$

When the map $T_0(\varepsilon)$ is written in the coordinates of Lemma 1, we say that it is in *the main normal form*. The identities (13) imply that map T_0 becomes both linear on $W_{loc}^u = \{x = 0, u = 0\}$, i.e. the restriction $T_0|_{W_{loc}^u}$ has a form $\bar{y} = \gamma(\varepsilon)y$, and linear in x on $W_{loc}^s = \{y = 0\}$, i.e. the restriction $T_0|_{W_{loc}^s}$ has a form $\bar{x} = A_1(\varepsilon)x$, $\bar{u} = A_2(\varepsilon)u + g_2(x, u, 0, \varepsilon)$. The latter also means that the strong stable foliation \mathcal{F}^{ss} is straightened, i.e., its leaves take the form $\mathcal{F}^s : \{x = \text{const}, y = 0\}$. It is important that when T_0 is brought to this normal form, the iterations $T_0^k : U_0 \rightarrow U_0$ of the local map do not differ too much from the iterations of the linearized map at all large k . Let $(x_k, u_k, y_k) = T_0^k(x_0, u_0, y_0)$. It has been known since [50] (see also [51, 52]) that (x_k, u_k, y_0) are uniquely defined functions of (x_0, u_0, y_k) for any $k \geq 0$.

Lemma 2. [28] *When the local map T_0 is brought to the main normal form, the following relations hold for all small ε and all large k :*

$$\begin{aligned} x_k - A_1^k(\varepsilon)x_0 &= \hat{\lambda}^k g_k(x_0, u_0, y_k, \varepsilon), & u_k &= \hat{\lambda}^k \hat{g}_k(x_0, u_0, y_k, \varepsilon), \\ y_0 - \gamma^{-k}(\varepsilon)y_k &= \hat{\gamma}^{-k} h_k(x_0, u_0, y_k, \varepsilon), \end{aligned} \quad (15)$$

where $\hat{\lambda}$ and $\hat{\gamma}$ are some constants such that $0 < \hat{\lambda} < \lambda$, $\hat{\gamma} > \gamma$, and the functions g_k, h_k, \hat{g}_k are uniformly bounded for all k , along with the derivatives up to the order $(r - 2)$. The derivatives of order $(r - 1)$ are estimated as

$$\left\| \frac{\partial^{r-1}(x_k - A_1(\varepsilon)^k x_0, u_k)}{\partial^{r-1}(x_0, u_0, y_k, \varepsilon)} \right\| = o(\|\lambda_1\|^k), \quad \left\| \frac{\partial^{r-1}(y_0 - \gamma(\varepsilon)^{-k} y_k)}{\partial^{r-1}(x_0, u_0, y_k, \varepsilon)} \right\| = o(\|\gamma\|^{-k}), \quad (16)$$

while the derivatives of order r are estimated as

$$\|x_k, u_k, y_0\|_{C^r} = o(1)_{k \rightarrow \infty}; \quad (17)$$

these estimates do not include derivatives with more than $(r - 2)$ differentiations with respect to ε (such may not exist)³.

Different versions of this lemma, as well as similar results for the flows near a saddle equilibrium state, can be found in [53, 38, 37, 14].

In the coordinates of Lemma 1, we have $P_i^+ = (x_i^+, u_i^+, 0)$ and $P_i^- = (0, 0, y_i^-)$ ($i = 1, 2$). The neighborhoods Π_i^+ can be taken as

$$\begin{aligned} \Pi_i^+ &= \{|x - x_i^+| < \delta^+, \|u - u_i^+\| < \delta^+, |y| < \delta^+\}, \\ \Pi_i^- &= \{|x| < \delta^-, \|u\| < \delta^-, |y - y_i^-| < \delta^-\}. \end{aligned} \quad (18)$$

We may also find a convenient form for each global map, using the simplicity of tangencies.

³see Remark 1 to Lemma 5 in [28]

Lemma 3. [28] *If the corresponding homoclinic tangencies are quadratic and simple, then the Taylor expansion (near the point $P_i^-(x = 0, u = 0, y = y_i^-)$) for map $T_i(\mu_i)$ ($i = 1, 2$) can be written in the following form:*

$$\begin{aligned}\bar{x} - x_i^+ &= a_i x + b_i(y - y_i^-) + p_i u + \dots, \\ \bar{u} - u_i^+ &= \tilde{a}_i x + \tilde{b}_i(y - y_i^-) + \tilde{p}_i u + \dots, \\ \bar{y} &= \mu_i + c_i x + d_i(y - y_i^-)^2 + q_i u + \dots,\end{aligned}\tag{19}$$

where $d_i \neq 0$, the dots denote high order terms in the Taylor expansion, and in the saddle case $x \in \mathbb{R}$, $b_i \neq 0$, $c_i \neq 0$ and in the saddle-focus case $x = (x_1, x_2) \in \mathbb{R}^2$, $b_i = (b_{i1}, b_{i2})^\top$, $c_i = (c_{i1}, c_{i2})$ with $\|b_i\| \neq 0$, $\|c_i\| \neq 0$.

All the coefficients shown in (19) depend on the parameters μ (they are at least C^{r-2} in μ). In particular, (x_i^+, u_i^+) and y_i^- are also ε -dependent, and at $\mu = 0$ they coincide with the coordinates of the homoclinic points P_i^+ and P_i^- , respectively.

We make some quick comments to this lemma which may be useful for the reader. First, for $\mu_i = 0$, formula (19) shows that $T_i(P_i^-) = P_i^+$. The manifold W_{loc}^u has equation $x = 0, y = 0$, hence, $T_i W_{loc}^u$ has the equation $\bar{x} - x_i^+ = (y - y_i^-)(b_i + \dots)$, $\bar{u} - u_i^+ = (y - y_i^-)(\tilde{b}_i + \dots)$, $\bar{y} = \mu_i + (y - y_i^-)^2(d_i + \dots)$. It follows that the tangency (at $\mu_i = 0$) is quadratic if $d_i \neq 0$, and this tangency split generally when varying μ_i . The equation of the tangent space $\mathcal{T}_{P_i^-} W_{loc}^{ue}$ is $u = 0$. At $\mu_i = 0$, the plane $DT_i(\mathcal{T}_{P_i^-} W_{loc}^{ue})$ has the equation $\bar{x} - x_i^+ = a_i x + b_i(y - y_i^-)$, $\bar{u} - u_i^+ = \tilde{a}_i x + \tilde{b}_i(y - y_i^-)$, $\bar{y} = c_i x$. The condition of simple tangency means that this plane intersects with the leaf $(x = x_i^+, y = 0)$ of the foliation \mathcal{F}^{ss} exactly in one point. Thus, the system $0 = a_i x + b_i(y - y_i^-)$, $0 = c_i x$ has $\{x = y = 0\}$ as its unique solution. This implies that $\|b_i\| \neq 0$, $\|c_i\| \neq 0$.

3.1 Rescaling lemma

Now we consider the first-return map T_{km} for a (k, m) -orbit; that is, for any point $(x_{02}, u_{02}, y_{02}) \in \Pi_2^+$ satisfying $T_{km}(x_{02}, u_{02}, y_{02}) = (\bar{x}_{02}, \bar{u}_{02}, \bar{y}_{02})$, we have (see Fig. 11)

$$(x_{02}, u_{02}, y_{02}) \xrightarrow{T_0^k} (x_{11}, u_{11}, y_{11}) \xrightarrow{T_1} (x_{01}, u_{01}, y_{01}) \xrightarrow{T_0^m} (x_{12}, u_{12}, y_{12}) \xrightarrow{T_2} (\bar{x}_{02}, \bar{u}_{02}, \bar{y}_{02}).\tag{20}$$

Note that by formula (15) the ordinate y_{02} is a function of (x_{02}, u_{02}, y_{11}) . Hence, we can study the map T_{km} in the so-called cross-coordinates [50], i.e. we represent it as $T_{km} : (x_{02}, u_{02}, y_{11}) \mapsto (\bar{x}_{02}, \bar{u}_{02}, \bar{y}_{11})$.

We first assume that $k \geq m$. Let $\Pi_{i,x,u}^+$ be the projection of Π_i^+ to the x, u -plane and $\Pi_{i,y}^-$ be the projection of Π_i^- to the y -axis (see (18)).

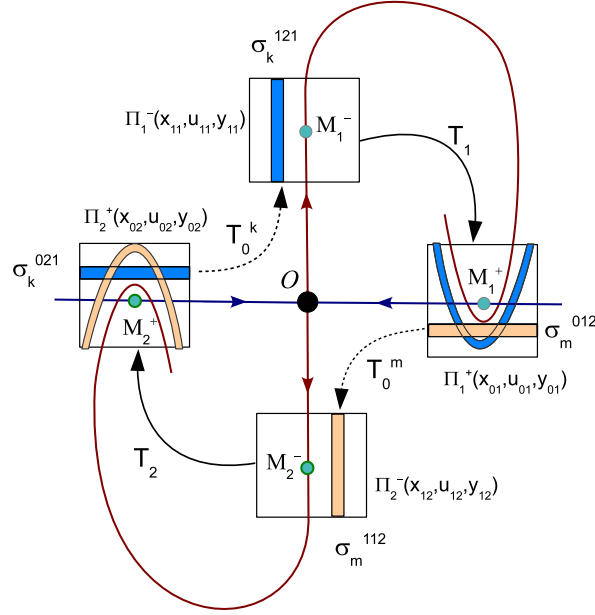


Figure 11: The action of T_{km} with associated coordinates at some non-zero μ value.

Lemma 4. Consider the first return map T_{km} in accordance with relation (20) with $k \geq m$. There exists a linear coordinate transformation $(x_{02}, u_{02}, y_{11}) \mapsto (X_2, U_2, Y_1)$ such that, in the new coordinates, the map T_{km} takes the form

$$\begin{aligned} \bar{X}_{21} &= M_1 - Y_1^2 + \phi_1(X_2, U_2, Y_1), \\ \bar{Y}_1 &= M_2 - \bar{X}_{21}^2 + C_2 \lambda^m \gamma^k Y_1 + \phi_2(X_2, U_2, Y_1), \\ (\bar{X}_{22}, U_2) &= \phi_3(X_2, U_2, Y_1), \end{aligned} \quad (21)$$

where in the saddle case the coordinate X_{22} is absent, $\lambda = \lambda_1$ and $C_2 = b_1 c_2$; in the saddle-focus case

$$C_2 = \sqrt{(b_{11}^2 + b_{12}^2)(c_{21}^2 + c_{22}^2)} \cdot \cos(m\varphi - \nu) \quad (22)$$

with ν given by

$$\sin \nu = \frac{b_{11}c_{22} - b_{12}c_{21}}{C_2} \quad \text{and} \quad \cos \nu = \frac{b_{11}c_{21} + b_{12}c_{22}}{C_2}.$$

The rescaled parameters $M_{1,2}$ are given by

$$\begin{aligned} M_1 &= -\sqrt[3]{d_1 d_2^2 \gamma^{\frac{4m+2k}{3}}} (\mu_1 - \gamma^{-m} y_2^- + O(\lambda^k + \hat{\gamma}^{-m})), \\ M_2 &= -\sqrt[3]{d_2 d_1^2 \gamma^{\frac{4k+2m}{3}}} (\mu_2 + \alpha_2 \lambda^m - \gamma^{-k} y_1^- + O(\hat{\lambda}^m + \hat{\gamma}^{-k})), \end{aligned} \quad (23)$$

where in the saddle case $\alpha_1 = c_1 x_2^+$; in the saddle-focus case $\alpha_2 = \tilde{C} \lambda^m \cos(m\varphi + \tilde{\beta})$, where

$$\tilde{C} = \sqrt{(c_{21}^2 + c_{22}^2)((x_{11}^+)^2 + (x_{12}^+)^2)}, \quad \sin \tilde{\beta} = \frac{c_{21}x_{12}^+ - c_{22}x_{11}^+}{\tilde{C}}, \quad \cos \tilde{\beta} = \frac{c_{21}x_{11}^+ + c_{22}x_{12}^+}{\tilde{C}}.$$

The functions ϕ_i satisfy

$$\begin{aligned}\phi_1(X_2, U_2, Y_1) &= \lambda^m \gamma^k O(\gamma^{-(2k+m)/3}) + O(\gamma^{-(2k+m)/3}), \\ \phi_2(X_2, U_2, Y_1) &= \lambda^m \gamma^k O\left(\delta_{km} + (\hat{\lambda}/\lambda)^m + \gamma^{-(2k+m)/3}\right) + O(\gamma^{-(2k+m)/3}) + (\hat{\gamma}/\gamma)^{-k}, \\ \phi_3(X_2, U_2, Y_1) &= \lambda^m \gamma^k O(\delta_{km}^{-1} \gamma^{-(2k+m)/3}) + O(\delta_{km}^{-1} \gamma^{-(2k+m)/3}),\end{aligned}\tag{24}$$

and their derivatives up to r with respect to variables and up to $(r-2)$ with respect to parameters also satisfy the above estimation. The coefficient δ_{km} is a freely chosen function of m and k such that $\delta_{km} \rightarrow 0$ as $k, m \rightarrow +\infty$.

Moreover, when (x_{02}, u_{02}, y_{11}) runs over $\Pi_{2,x,u}^+ \times \Pi_{1,y}^-$, the new coordinates cover a centered at zero ball in \mathbb{R}^{n+1} whose radius grows to infinity as $k, m \rightarrow \infty$.

We give the proof of Lemma 4 in Section 5. Analogous results hold in the case $k < m$. This is done by considering symmetrically for map T_{km} in the form $T_{km} = T_1 T_0^k T_2 T_0^m$, i.e, in accordance with relation

$$(x_{01}, u_{01}, y_{01}) \xrightarrow{T_0^m} (x_{12}, u_{12}, y_{12}) \xrightarrow{T_2} (x_{02}, u_{02}, y_{02}) \xrightarrow{T_0^k} (x_{11}, u_{11}, y_{11}) \xrightarrow{T_1} (\bar{x}_{01}, \bar{u}_{01}, \bar{y}_{01}),\tag{25}$$

when we take the starting point in Π_1^+ , see Fig. 11. Then the proof is conducted in the same way as for Lemma 4 with evident exchanges between coordinates and parameters. Therefore, we formulate the following result without the proof.

Lemma 5. Consider the first return map T_{km} in accordance with relation (25) with $k < m$. There exists a linear coordinate transformation $(x_{01}, u_{01}, y_{12}) \mapsto (X_1, U_1, Y_2)$ such that, in the new coordinates, the map T_{km} takes the form

$$\begin{aligned}\bar{X}_{11} &= M_2 - Y_2^2 + \psi_1(X_2, U_2, Y_1), \\ \bar{Y}_2 &= M_1 - \bar{X}_{11}^2 + C_1 \lambda^k \gamma^m Y_2 + \psi_2(X_2, U_2, Y_1), \\ (\bar{X}_{12}, U_1) &= \psi_3(X_2, U_2, Y_1),\end{aligned}\tag{26}$$

where in the saddle case the coordinate X_{12} is absent, $\lambda = \lambda_1$ and $C_1 = b_{2c_1}$; in the saddle-focus case

$$C_1 = \sqrt{(b_{21}^2 + b_{22}^2)(c_{11}^2 + c_{12}^2)} \cdot \cos(k\varphi - \tilde{\nu})\tag{27}$$

with $\hat{\nu}$ given by

$$\sin \hat{\nu} = \frac{b_{21}c_{12} - b_{22}c_{11}}{C_1} \quad \text{and} \quad \cos \hat{\nu} = \frac{b_{21}c_{11} + b_{22}c_{12}}{C_1}.$$

The rescaled parameters $M_{1,2}$ are given by

$$\begin{aligned}M_1 &= -\sqrt[3]{d_1 d_2^2 \gamma^{\frac{4m+2k}{3}}} \left(\mu_1 - \gamma^{-m} y_2^- + \alpha_1 \lambda^k + O(\hat{\lambda}^k + \hat{\gamma}^{-m}) \right), \\ M_2 &= -\sqrt[3]{d_2 d_1^2 \gamma^{\frac{4k+2m}{3}}} \left(\mu_2 - \gamma^{-k} y_1^- + O(\lambda^m + \hat{\gamma}^{-k}) \right),\end{aligned}\tag{28}$$

where in the saddle case $\alpha_1 = c_1 x_2^+$; in the saddle-focus case $\alpha_1 = \hat{C} \lambda^k \cos(k\varphi + \hat{\beta})$, where

$$\hat{C} = \sqrt{(c_{11}^2 + c_{12}^2)((x_{21}^+)^2 + (x_{22}^+)^2)}, \quad \sin \hat{\beta} = \frac{c_{11}x_{22}^+ - c_{12}x_{21}^+}{\hat{C}}, \quad \cos \hat{\beta} = \frac{c_{11}x_{21}^+ + c_{12}x_{22}^+}{\hat{C}}.$$

The functions ψ_i satisfy

$$\begin{aligned} \psi_1(X_2, U_2, Y_1) &= \lambda^k \gamma^m O(\gamma^{-(2m+k)/3}) + O(\gamma^{-(2m+k)/3}), \\ \psi_2(X_2, U_2, Y_1) &= \lambda^k \gamma^m O(\delta_{km} + (\hat{\lambda}/\lambda)^k + \gamma^{-(2m+k)/3}) + O(\gamma^{-(2m+k)/3}) + (\hat{\gamma}/\gamma)^{-m}, \\ \psi_3(X_2, U_2, Y_1) &= \lambda^k \gamma^m O(\delta_{km}^{-1} \gamma^{-(2m+k)/3}) + O(\delta_{km}^{-1} \gamma^{-(2m+k)/3}), \end{aligned}$$

whose derivatives satisfy estimates similar to those for (24).

Moreover, when (x_{01}, u_{01}, y_{12}) runs over $\Pi_{1,x,u}^+ \times \Pi_{2,y}^-$, the new coordinates cover a centered at zero ball in \mathbb{R}^{n+1} whose radius grows to infinity as $k, m \rightarrow \infty$,

4 Proofs of Theorems 1 and 2.

4.1 Proof of Theorem 1

We prove the theorem for the $k \geq m$ case and the other follows by a similar argument (we can consider the map $T_{mk} = T_0^k T_1 T_0^m T_2$ instead). We do not assume here that the homoclinic tangencies are simple. Nevertheless, we can consider in U_0 local C^r -coordinates $(x, y) \in R^n \times R$ in which the local stable and unstable invariant manifolds W_{loc}^s and W_{loc}^u of the point O are straightened, i.e., the local map $T_0(\mu)$ has the form:

$$T_0 : \bar{x} = A(\mu)x + g(x, y, \mu), \quad \bar{y} = \gamma y + h(x, y, \mu),$$

where the matrix A has the eigenvalues $\lambda_1, \dots, \lambda_n$ such that $1 > |\lambda_1| \geq \dots \geq |\lambda_n| > 0$; and $f(0, y, \mu) \equiv 0, g(x, 0, \mu) \equiv 0$. Since y is one-dimensional and $|\lambda_1||\gamma| < 1$, we can assume [28] that additionally the identities $h(0, y, \mu) \equiv 0, h_y(x, 0, \mu) \equiv 0$ are fulfilled. Then we can apply Lemma 2, where the coordinate u is omitted and $\|A\| = \lambda = |\lambda_1| + \epsilon_0$ with arbitrary small constant $\epsilon_0 \geq 0$. Then the global maps $T_1 \equiv f^{N_1} : \Pi_1^- \rightarrow \Pi_1^+$ and $T_2 \equiv f^{N_2} : \Pi_2^- \rightarrow \Pi_2^+$ can be written in the form

$$\begin{aligned} \bar{x}_{0i} - x_i^+ &= F_i(x_{1i}, y_{1i} - y_i^-, \mu), \\ \bar{y}_{0i} &= G_i(x_{1i}, y_{1i} - y_i^-, \mu), \quad i = 1, 2, \end{aligned}$$

where $F_i(0, 0, 0) = 0, G_i(0, 0, 0) = 0$, which means that $T_i(P_i^-) = P_i^+$ at $\mu = 0$, and $\partial G_i / \partial y(0, 0, 0) = 0, \partial^2 G_i / \partial y^2(0, 0, 0) = 2d_i \neq 0$, which means that $W^u(O)$ and $W^s(O)$ have at $\mu = 0$ the quadratic homoclinic tangencies at the points of the homoclinic orbits

Γ_1 and Γ_2 . Thus, we can write the function G_i in the form $G_i = \mu_i + C(x_{1i}) + d_i(y_{1i} - y_i^-)^2 + O(\|x_{1i}\| |y_{1i} - y_i^-| + |y_{1i} - y_i^-|^3)$

Now we can write the first-return map $T_{km} : \Pi_2^+ \rightarrow \Pi_2^+$, by virtue of the composition (20), see Fig. 11), assuming that $k \geq m$. :

$$x_{01} - x_1^+ = F_1(x_{11}, y_{11} - y_1^-, \mu), \quad y_{01} = G_1(x_{11}, y_{11} - y_1^-, \mu),$$

where $x_{11} = \lambda^k \varphi_k^1(x_{02}, y_{11}, \mu)$, $y_{01} = \gamma^{-m} y_{11} + \gamma^{-2m} \varphi_k^2(x_{02}, y_{11}, \mu)$,

$$\bar{x}_{02} - x_2^+ = F_2(x_{12}, y_{12} - y_2^-, \mu), \quad \bar{y}_{02} = G_2(x_{12}, y_{12} - y_2^-, \mu),$$

where $x_{12} = \lambda^m \varphi_m^1(x_{01}, \bar{y}_{11}, \mu)$, $\bar{y}_{02} = \gamma^{-k} \bar{y}_{11} + \gamma^{-2k} \varphi_k^2(\bar{x}_{02}, \bar{y}_{11}, \mu)$,

Shifting the coordinates $x_i = x_{0i} - x_i^+$, $y_i = y_{1i} - y_i^-$ we bring map T_{km} to the form

$$\begin{aligned} x_1 &= O(\lambda^k) + O(y_1), \\ \gamma^{-m} y_2 &= \hat{\mu}_1 + d_1 y_1^2 + \lambda^k O(\|x\|) + \gamma^{-2k} O(y_1) + O(y_1^3), \\ \bar{x}_2 &= O(\lambda^m) + O(y_2), \\ \gamma^{-k} \bar{y}_1 &= \hat{\mu}_2 + d_2 y_2^2 + \lambda^m O(\|x\|) + \gamma^{-2m} O(y_2) + O(y_2^3), \end{aligned} \tag{29}$$

Now we rescale the coordinates as follows

$$y_1 = \beta_1 Y_1, \quad y_2 = \beta_2 Y_2, \quad X_1 = \rho_k^{-1} \beta_1 X_1, \quad X_2 = \rho_m^{-1} \beta_2 X_2$$

where

$$\beta_1 = -\frac{1}{\sqrt[3]{d_2 d_1^2}} \gamma^{-\frac{k}{3}} \gamma^{-\frac{2m}{3}}, \quad \beta_2 = -\frac{1}{\sqrt[3]{d_1 d_2^2}} \gamma^{-\frac{m}{3}} \gamma^{-\frac{2k}{3}},$$

and ρ_i is a function of i which tends to 0 as $i \rightarrow +\infty$. After this, map (29) takes the form

$$\begin{aligned} X_1 &= O(\lambda^k \gamma^{(k+2m)/3}) + O(\rho_k), \\ Y_2 &= M_1 - Y_1^2 + O(\lambda^k \gamma^m \rho_k^{-1}) + O(\gamma^{-(k+2m)/3}) + O(\gamma^{-(2k+m)/3}), \\ \bar{X}_2 &= O(\lambda^m \gamma^{(2k+m)/3}) + O(\rho_m), \\ \bar{Y}_1 &= M_2 - Y_2^2 + O(\lambda^m \gamma^k \rho_m^{-1}) + O(\gamma^{-(k+2m)/3}) + O(\gamma^{-(2k+m)/3}). \end{aligned} \tag{30}$$

The statement on the ranges of the rescaled coordinates and parameters is immediate from (30), so we only need to prove that the quantity

$$S_{km} = |\lambda|^m |\gamma|^k \tag{31}$$

converges to zero as $k, m \rightarrow \infty$. Let $\hat{\theta} = -\ln |\lambda| / \ln |\gamma|$, hence $|\lambda| = |\gamma|^{-\hat{\theta}}$. If $k \geq m$, condition (4) means that $(\hat{\theta} - \delta_1)^{-1} < m/k < 1$, i.e. $k < m(\hat{\theta} - \delta_1)$, with some small $\delta_1 > 0$. Then

$$S_{km} = |\gamma|^{k-m\hat{\theta}} \geq |\gamma|^{m(\hat{\theta}-\delta_1)-m\hat{\theta}} = |\gamma|^{-m\delta_1} \rightarrow 0 \quad \text{as } m \rightarrow \infty.$$

4.2 Proof of Theorem 2.

We only prove for the case where $k \geq m$ using Lemma 4; when $k < m$, similar argument applies with using Lemma 5 instead of Lemma 4.

Let us start with the saddle case. By Lemma 4, we need to find a sequence $\{(k_j, m_j)\}$ of positive integers with $k_j \geq m$ and $k_j, m_j \rightarrow +\infty$ as $j \rightarrow +\infty$ such that, when $\mu_3 = \theta - \theta_0$ varies near 0, the coefficients $C_2 \lambda^{m_j} \gamma^{k_j}$ of Y_1 in (21) can cover either $[-s_j, -s_j^{-1}]$ or $[s_j^{-1}, s_j]$ for some sequence $\{s_j\}$ of positive numbers tending to infinity.

Evidently, since $C_2 = b_1 c_2 \neq 0$ is a constant, it is sufficient to check that the function $S_j = |\lambda|^{m_j} |\gamma|^{k_j}$ as $j \rightarrow +\infty$ approximate the infinite interval $(0, +\infty)$ when values of θ runs over an (arbitrary small) neighborhood of θ_0 .

We have for $\ln S_j$ that

$$\theta = \frac{k_j}{m_j} - \frac{\ln S_j}{m_j \ln |\gamma|}. \quad (32)$$

Take any sequence $\{s_j\}$ of positive numbers with $s_j \rightarrow \infty$ as $j \rightarrow \infty$. Let θ_j^1 and θ_j^2 be the corresponding values of θ at $S_j = s_j^{-1}$ and $S_j = s_j$. Then

$$\theta_j^{1,2} = \frac{k_j}{m_j} \mp \frac{\ln s_j}{m_j \ln |\gamma|}.$$

So, when θ runs over the interval $[\theta_j^1, \theta_j^2]$, the values of S_j cover $[s_j^{-1}, s_j]$. Let

$$I_j = [\min(\theta_j^1, \theta_0), \max(\theta_j^2, \theta_0)].$$

We will find the desired sequence $\{(k_j, m_j)\}$ if $\text{diam } I_j \rightarrow 0$ as $j \rightarrow \infty$. This can be easily achieved by taking m_j, k_j such that

$$\frac{k_j}{m_j} \rightarrow \theta_0 \quad \text{and} \quad \frac{\ln s_j}{m_j \ln |\gamma|} \rightarrow 0$$

as $j \rightarrow \infty$.

The statement on the parameters $\mu_{1,2}$ and $M_{1,2}$ follows immediately from (23). The proof for the saddle case will be completed if the functions ϕ_i ($i = 1, 2, 3$) in (21) along with their derivatives tend to 0 as $j \rightarrow +\infty$. This gives us only some restriction for the exponential growth of $\lambda^m \gamma^k$, which, by (24), is equivalent to require

$$\lambda^m \gamma^k < \max\{\delta_{km} \gamma^{(2k+m)/3}, \delta_{km}^{-1}, (\hat{\lambda}/\lambda)^{-m}\}.$$

This inequality can be readily fulfilled by taking appropriate δ_{km} .

We proceed to consider the saddle-focus case. According to (22), the coefficient $C_2 \lambda^{m_j} \gamma^{k_j}$ in (21) now has the form

$$C_j := C \cos(m_j \varphi - \nu) \lambda^{m_j} \gamma^{k_j}, \quad (33)$$

where $C = \sqrt{(b_{11}^2 + b_{12}^2)(c_{21}^2 + c_{22}^2)}$. The idea here is the same as in the saddle case, i.e., we find a sequence $\{(k_j, m_j)\}$ of positive integers with $k_j \geq m$ and $k_j, m_j \rightarrow +\infty$ as $j \rightarrow +\infty$ such that by changing the parameter μ_3 the values of C_j can cover the whole real line in the limit. The difference is that we now vary φ , instead of θ , near φ_0 such that the value of $\cos(m_j\varphi - \nu)$ is close to zero, and, at the same time, have $\lambda^{m_j}\gamma^{k_j} \rightarrow \infty$ as $k, m \rightarrow \infty$.

Take any sequence $\{s_j\}$ of positive numbers with $s_j \rightarrow \infty$ as $j \rightarrow \infty$. Recall that the range of \arccos is $[0, \pi]$. We solve out φ from the equations

$$\cos(m_j\phi_j^{1,2} - \nu) = \pm \frac{s_j}{C\lambda^{m_j}\gamma^{k_j}}$$

as

$$\begin{aligned}\varphi_j^1 &= \frac{1}{m_j} \left(\arccos \frac{s_j}{C\lambda^{m_j}\gamma^{k_j}} - \nu - \frac{2\pi n_j}{m_j} \right), \\ \varphi_j^2 &= \frac{1}{m_j} \left(\pi - \arccos \frac{s_j}{C\lambda^{m_j}\gamma^{k_j}} - \nu - \frac{2\pi n_j}{m_j} \right),\end{aligned}\tag{34}$$

where n_j can be any integers. Hence, when φ runs over

$$I_j = [\min(\varphi_j^1, \varphi_0), \max(\varphi_j^2, \varphi_0)],$$

the values of C cover the interval $[-s_j, s_j]$.

We now choose n_j and m_j such that

$$\frac{n_j}{m_j} \rightarrow \frac{\varphi_0}{2\pi} \quad \text{as } j \rightarrow \infty,$$

and, then, choose $k_j \geq m_j$ accordingly so that

$$\frac{s_j}{C\lambda^{m_j}\gamma^{k_j}} \rightarrow 0 \quad \text{as } j \rightarrow \infty.$$

In this way, we find from (34) that $\text{diam } I_j \rightarrow 0$ as $j \rightarrow \infty$.

Arguing as in the saddle case, one achieves the statement on other parameters and shows that the functions ϕ_i ($i = 1, 2, 3$) converge to 0 as $j \rightarrow \infty$. \square

5 Proof of Lemma 4

As mentioned before, we study the cross-form of the map T_{km} according to (20). Using formulas (15) and (19) we can write the relation (20) as

$$\begin{aligned}(x_{11} - A_1^k x_{02}, u_{11}) &= \hat{\lambda}^k (g_k(x_{02}, u_{02}, y_{11}, \varepsilon), \hat{g}_k(x_{02}, u_{02}, y_{11}, \varepsilon)), \\ \bar{y}_{02} &= \gamma^{-k} \bar{y}_{11} + \hat{\gamma}^{-k} h_k(\bar{x}_{02}, \bar{u}_{02}, \bar{y}_{11}, \varepsilon),\end{aligned}\tag{35}$$

$$\begin{aligned}
x_{01} - x_1^+ &= a_1 x_{11} + b_1 (y_{11} - y_1^-) + p_1 u_{11} + \dots, \\
u_{01} - u_1^+ &= \tilde{a}_1 x_{11} + \tilde{b}_1 (y_{11} - y_1^-) + \tilde{p}_1 u_{11} + \dots, \\
y_{01} &= \mu_1 + c_1 x_{11} + d_1 (y_{11} - y_1^-)^2 + q_1 u_{11} + \dots,
\end{aligned} \tag{36}$$

$$\begin{aligned}
(x_{12} - A_1^m x_{01}, u_{12}) &= \hat{\lambda}^m (g_m(x_{01}, u_{01}, y_{12}, \varepsilon), \hat{g}_m(x_{01}, u_{01}, y_{12}, \varepsilon)), \\
y_{01} &= \gamma^{-m} y_{12} + \hat{\gamma}^{-m} h_m(x_{01}, u_{01}, y_{12}, \varepsilon),
\end{aligned} \tag{37}$$

$$\begin{aligned}
\bar{x}_{02} - x_2^+ &= a_2 x_{12} + b_2 (y_{12} - y_2^-) + p_2 u_{12} + \dots, \\
\bar{u}_{02} - u_2^+ &= \tilde{a}_2 x_{12} + \tilde{b}_2 (y_{12} - y_2^-) + \tilde{p}_2 u_{12} + \dots, \\
\bar{y}_{02} &= \mu_2 + c_2 x_{12} + d_2 (y_{12} - y_2^-)^2 + q_2 u_{12} + \dots.
\end{aligned} \tag{38}$$

We construct the sought linear change of coordinates in several steps.

Step 1. We shift the coordinates with

$$x_i = x_{0i} - x_i^+, \quad u_i = u_{0i} - u_i^+, \quad y_i = y_{1i} - y_i^-, \quad i = 1, 2.$$

Then

$$\begin{aligned}
x_{11} &= A_1^k x_2 + A_1^k x_2^+ + O(\hat{\lambda}^k), \quad u_{11} = O(\hat{\lambda}^k), \quad y_{02} = \gamma^{-k} y_1 + \gamma^{-k} y_1^- + O(\tilde{\gamma}^{-k}), \\
x_{12} &= A_1^m x_1 + A_1^m x_1^+ + O(\hat{\lambda}^m), \quad u_{12} = O(\hat{\lambda}^m), \quad y_{01} = \gamma^{-m} y_2 + \gamma^{-m} y_2^- + O(\tilde{\gamma}^{-m}),
\end{aligned}$$

and the system (35)–(38) recasts as (recall that $k \geq m$)

$$\begin{aligned}
x_1 &= b_1 y_1 + O(\lambda^k) + O(y_1^2), \\
u_1 &= \tilde{b}_1 y_1 + O(\lambda^k) + O(y_1^2), \\
\gamma^{-m} y_2 &= \tilde{\mu}_1 + d_1 y_1^2 + \lambda^k O(\|(x_2, u_2)\|) + O(|y_1| \|(x_2, u_2)\| + |y_1|^3), \\
\bar{x}_2 &= b_2 y_2 + O(\lambda^m) + O(y_2^2), \\
\bar{u}_2 &= \tilde{b}_2 y_2 + O(\lambda^m) + O(y_2^2), \\
\gamma^{-k} \bar{y}_1 &= \tilde{\mu}_2 + d_2 y_2^2 + C_2 A_1^m x_1 + \hat{\lambda}^m O(\|(x_1, u_1)\|) + O(\lambda^m |y_2| \|(x_1, u_1)\| + |y_2|^3),
\end{aligned} \tag{39}$$

where $C_2 A_1^m x_1 = c_2 \lambda^m x_1$ in the saddle case, $C_2 A_1^m x_1 = (c_{21}, c_{22}) A_1^m (x_{11}, x_{12})^\top$ in the saddle-focus case),

$$\begin{aligned}
\tilde{\mu}_1 &= \mu_1 - \gamma^{-m} y_2^- + O(\lambda^k + \hat{\gamma}^{-m}), \\
\tilde{\mu}_2 &= \mu_2 - \gamma^{-k} y_2^- + \alpha_2 \lambda^m + O(\lambda^k + \hat{\gamma}^{-k} + \hat{\lambda}^m)
\end{aligned}$$

and α_2 is the same as in the statement of Lemma 4.

Step 2. The above coordinate transformation gives rise to constant terms in the equations for x_1, u_1, \bar{x}_2 and \bar{u}_2 , and to linear-in- y_1 and linear-in- y_2 terms in equations for y_2 and \bar{y}_1 , respectively. In order to kill those terms, we shift the coordinates further with

$$(x_1, u_1, y_1) \mapsto (x_1, u_1, y_1) + O(\lambda^k), \quad (x_2, u_2, y_2) \mapsto (x_2, u_2, y_2) + O(\lambda^m),$$

where the terms $O(\lambda^k)$ and $O(\lambda^m)$ are chosen appropriately. After that, the formula (39) can be rewritten as

$$\begin{aligned}
x_1 &= b_1 y_1 + \lambda^k O(\|(x_2, u_2)\|) + O(y_1^2), \\
u_1 &= \tilde{b}_1 y_1 + \lambda^k O(\|(x_2, u_2)\|) + O(y_1^2), \\
\gamma^{-m} \bar{y}_2 &= \tilde{\mu}_1 + d_1 y_1^2 + \lambda^k O(\|(x_2, u_2)\|) + O(\lambda^k |y_1| \|(x_2, u_2)\| + |y_1|^3), \\
\bar{x}_2 &= b_2 y_2 + \lambda^m O(\|(x_1, u_1)\|) + O(y_2^2), \\
\bar{u}_2 &= \tilde{b}_2 y_2 + \lambda^m O(\|(x_1, u_1)\|) + O(y_2^2), \\
\gamma^{-k} \bar{y}_1 &= \tilde{\mu}_2 + d_2 y_2^2 + C_2 A_1^m x_1 + \hat{\lambda}^m O(\|(x_1, u_1)\|) + O(\lambda^m |y_2| \|(x_1, u_1)\| + |y_2|^3),
\end{aligned} \tag{40}$$

Step 3. We apply affine transformation for (x, u) -coordinates. In the saddle case we put, since $b_1 b_2 \neq 0$,

$$u_i^{new} = u_i - \frac{\tilde{b}_i}{b_i} x_i, \quad i = 1, 2.$$

In the saddle-focus case, when $x_i = (x_{i1}, x_{i2})$, $b_i = (b_{i1}, b_{i2})$ and $b_{i1}^2 + b_{i2}^2 \neq 0$ ($i = 1, 2$), we assume, without loss of generality, that $b_{11} \neq 0$ and $b_{21} \neq 0$. We put

$$x_{i2}^{new} = x_{i2} - \frac{b_{i2}}{b_{i1}} x_{i1}, \quad u_i^{new} = u_i - \frac{\tilde{b}_i}{b_{i1}} x_{i1}, \quad i = 1, 2.$$

Then, system (40) takes the form as

$$\begin{aligned}
x_{11} &= b_{11} y_1 + \lambda^k O(\|(x_2, u_2)\|) + O(y_1^2), \\
(x_{12}, u_1) &= \lambda^k O(\|(x_2, u_2)\|) + O(y_1^2), \\
\gamma^{-m} \bar{y}_2 &= \tilde{\mu}_1 + d_1 y_1^2 + \lambda^k O(\|(x_2, u_2)\|) + O(\lambda^k |y_1| \|(x_2, u_2)\| + |y_1|^3), \\
\bar{x}_{21} &= b_{21} y_2 + \lambda^m O(\|(x_1, u_1)\|) + O(y_2^2), \\
(\bar{x}_{22}, \bar{u}_2) &= \lambda^k O(\|(x_1, u_1)\|) + O(y_2^2), \\
\gamma^{-k} \bar{y}_1 &= \tilde{\mu}_2 + d_2 y_2^2 + \tilde{C}_2 \lambda^m x_1 + \hat{\lambda}^m O(\|(x_1, u_1)\|) + O(\lambda^m |y_2| \|(x_1, u_1)\| + |y_2|^3),
\end{aligned} \tag{41}$$

where in the saddle case the coordinates x_{12} and x_{22} are absent, and $x_{11} = x_1, x_{21} = x_2$ and $\tilde{C}_2 = c_2$; in the saddle-focus case $\tilde{C}_2 x_2 = \tilde{C}_{21} x_{21} + \tilde{C}_{22} x_{22}$, where

$$\tilde{C}_{21} = \frac{1}{b_{21}} \sqrt{(b_{21}^2 + b_{22}^2)(c_{21}^2 + c_{22}^2)} \cdot \cos(m\varphi - \nu), \quad \nu = \arctan \frac{b_{21}c_{22} - b_{22}c_{21}}{b_{21}c_{21} + b_{22}c_{22}}$$

and $\tilde{C}_{22} = \sqrt{c_{21}^2 + c_{22}^2} \cos(m\varphi + \tilde{\nu})$, with $\tilde{\nu} = \arctan(c_{21}/c_{22})$.

Step 4. Now we rescale the coordinates in system (41) as follows:

$$\begin{aligned}
y_1 &= \beta_1 Y_1, & x_{11} &= b_{11} \beta_1 X_1, & (x_{12}, u_1) &= \tilde{\delta}_{km} \beta_1 (X_{12}, U_1) \\
y_2 &= \beta_2 Y_2, & x_{21} &= b_{21} \beta_2 X_2, & (x_{22}, u_2) &= \delta_{km} \beta_2 (X_{22}, U_2)
\end{aligned} \tag{42}$$

where

$$\beta_1 = -\frac{1}{\sqrt[3]{d_2 d_1^2}} \gamma^{-\frac{k}{3}} \gamma^{-\frac{2m}{3}}, \quad \beta_2 = -\frac{1}{\sqrt[3]{d_1 d_2^2}} \gamma^{-\frac{m}{3}} \gamma^{-\frac{2k}{3}}, \quad (43)$$

and $\tilde{\delta}_{km}$ and δ_{km} are some functions of m and k which tend to 0 as $k, m \rightarrow +\infty$.

Then system (41) recasts as

$$\begin{aligned} X_{11} &= Y_1 + O(\lambda^k \gamma^{-(k-m)/3}) + O(\gamma^{-(k+2m)/3}), \\ (X_{12}, U_1) &= \tilde{\delta}_{km}^{-1} O(\lambda^k \gamma^{-(k-m)/3}) + \delta_{km}^{-1} O(\gamma^{-(k+2m)/3}), \\ Y_2 &= M_1 - Y_1^2 + O(\lambda^k \gamma^m \gamma^{-(k-m)/3} + \hat{\gamma}^{-m} \gamma^m + \gamma^{-(k+2m)/3}), \\ \bar{X}_{21} &= Y_2 + O(\lambda^m \gamma^k \gamma^{-(2k+m)/3} + \gamma^{-(2k+m)/3}), \\ (\bar{X}_{22}, U_2) &= \delta_{km}^{-1} O(\lambda^m \gamma^k \gamma^{-(2k+m)/3}) + \delta_{km}^{-1} O(\gamma^{-(2k+m)/3}), \\ \bar{Y}_1 &= M_2 - Y_2^2 + C_2 \lambda^m \gamma^k X_{11} + \\ &\quad + \delta_{km} \lambda^m \gamma^k O(X_{12}) + O(\hat{\lambda}^m \gamma^k + \hat{\gamma}^{-k} \gamma^k + \lambda^m \gamma^k \gamma^{-(2k+m)/3} + \gamma^{-(2k+m)/3}), \end{aligned} \quad (44)$$

where $X_{11}, X_{21} \in \mathbb{R}$ and the coordinates X_{12} and X_{22} are absent in the saddle case. Since $k \geq m$, we can take, for example, $\tilde{\delta}_{km} = \gamma^{-k/3}$.

Finally, expressing intermediate coordinates (X_1, U_1, Y_2) from the first three equations of (44) and putting the result into the last three equations, we obtain the following form of T_{km}

$$\begin{aligned} \bar{X}_{21} &= M_1 - Y_1^2 + \lambda^m \gamma^k O(\gamma^{-(2k+m)/3}) + o(1)_{k,m \rightarrow +\infty}, \\ \bar{Y}_1 &= M_2 - \bar{X}_{21}^2 + C_2 \lambda^m \gamma^k Y_1 + \lambda^m \gamma^k O(\delta_{km} + (\hat{\lambda}/\lambda)^m + \gamma^{-(2k+m)/3}) + o(1)_{k,m \rightarrow +\infty}, \\ (\bar{X}_{22}, U_2) &= \lambda^m \gamma^k O(\delta_{km}^{-1} \gamma^{-(2k+m)/3}) + O(\delta_{km}^{-1} \gamma^{-(2k+m)/3}), \end{aligned} \quad (45)$$

The last statement of the lemma on the range of the new coordinates follows immediately from (42) and (43). \square

6 Acknowledgment

This paper was carried out in the framework of the RSciF Grant No. 19-11-00280 and partially supported by the grant 0729-2020-0036 of the Ministry of Science and Higher

Education of the Russian Federation (Section 3). S. Gonchenko thanks the Theoretical Physics and Mathematics Advancement Foundation BASIS, Grant No. 20-7-1-36-5, for support of scientific investigations of his group. D. Li was supported by ERC project 677793 StableChaoticPlanetM.

References

- [1] J.A.C. Gallas, Structure of the parameter space of the Hénon map // Phys. Rev. Lett. 1993, v.70(18), 2714-2717.
- [2] J.A.C. Gallas, Dissecting Shrimps: Results for Some One-Dimensional Physical Models // Physica A, 1994, 202, 196-223.
- [3] B.R. Hunt, J.A.C. Gallas, C. Grebogi, J.A. Yorke, H. Kocak, Bifurcation rigidity // Physica D, 1999, 129, 35.
- [4] C. Bonatto, J.A.C. Gallas, Y. Ueda, Chaotic phase similarities and recurrences in a damped-driven Duffing oscillator // Phys. Rev. E, 2008, 77, 026217.
- [5] E.N. Lorenz, Compound windows of the Hénon-map // Physica D, 2008, v.237, 1689-1704.
- [6] S.V. Gonchenko, On a two parameter family of systems close to a system with a nontransversal Poincaré homoclinic curve. I. // Methods of Qualitative Theory of Differential Equations; Ed. Gorky St. Univ., 1985, 55-72. English transl. in: Selecta Math. Sovietica, 1990, 10
- [7] H.R. Dullin, J.D. Meiss, Generalized Hénon maps: the cubic diffeomorphisms of the plane // Phys. D, 2000, v.143, 262-289.
- [8] M. Gonchenko, S.V. Gonchenko, I. Ovsyannikov, Bifurcations of Cubic Homoclinic Tangencies in Two-dimensional Symplectic Maps // Math. Modeling of Natural Phenomena // 2017, v.12(1).
- [9] C. Mirá, Chaotic Dynamics. From the One-Dimensional Endomorphism to the Two-dimensional Diffeomorphism // World Scientific, Singapore, 1987.
- [10] J.P. Carcasses, C. Mirá, M. Bosh, C. Simo, J.C. Tatjer, “Crossroad area – spring area” transition (I) Parameter plane representation // Bifurcation and Chaos, 1991, v.1, No.1, 183-196.

- [11] J.P. Carcasses, C. Mirá, M. Bosch, C. Simo and J.C. Tatjer. “Crossroad area – spring area” transition (II). Foliated parametric representation // *Int. J. Bifur. and Chaos*, 1991, 1(2), 339- 348.
- [12] C. Mirá, J.P. Carcasses, “Crossroad area – saddle area” and “crossroad area – spring area” transitions // *Bifurcation and Chaos*, 1991, v.1, No.3, 641-655.
- [13] S.V. Gonchenko, I.I. Ovsyannikov, D.V. Turaev, On the effect of invisibility of stable periodic orbits at homoclinic bifurcations // *Physica D* 421, 2012, 1115-1122.
- [14] L.P. Shilnikov, A.L. Shilnikov, D.V. Turaev, L.O. Chua, *Methods of qualitative theory in nonlinear dynamics* // World Scientific, Part I., 1998; Part II, 2001.
- [15] S.E. Newhouse, The abundance of wild hyperbolic sets and non-smooth stable sets for diffeomorphisms // *Publ. Math. Inst. Hautes Etudes Sci.*, 1979, v.50, 101-151.
- [16] S.V. Gonchenko, D.V. Turaev, and L.P. Shilnikov, On the existence of Newhouse domains in a neighborhood of systems with a structurally unstable Poincaré homoclinic curve (the higher-dimensional case) // *Dokl. Math.*, 1993, 47 (2), 268-273.
- [17] J. Palis and M. Viana, High dimension diffeomorphisms displaying infinitely many periodic attractors // *Ann. Math., Ser. 2*, 1994, 140 (1), 207-250.
- [18] N. Romero, Persistence of homoclinic tangencies in higher dimensions // *Ergodic Theory Dyn. Syst.*, 1995, 15 (4), 735-757.
- [19] S.V. Gonchenko, D.V. Turaev and L.P. Shilnikov, On models with a structurally unstable homoclinic Poincaré curve // *Sov. Math., Dokl.* 44, 422-426 (1992).
- [20] Lai Y-C., Grebogi C., Yorke J.A., Kan I., How often are chaotic saddles nonhyperbolic // *Nonlinearity*, 1993, Vol. 6, No. 5, 779-797.
- [21] S.V. Gonchenko, L.P. Shilnikov and D.V. Turaev, On models with non-rough Poincaré homoclinic curves // *Physica D* 62, 1-14 (1993).
- [22] J. Palis, A Global View of Dynamics and a Conjecture on the Denseness of Finitude of Attractors // *Asterisque*, 2000, v. 261, pp. 339-351.
- [23] N.K. Gavrilov and L.P. Shilnikov, On three-dimensional dynamical systems close to systems with a structurally unstable homoclinic curve”.- Part 1 // *Math.USSR Sb.*, 1972, v.17, 467-485; Part 2 // *Math.USSR Sb*, 1973, v.19, 139-156.
- [24] S. E. Newhouse, Diffeomorphisms with infinitely many sinks // *Topology*, 1974, 13, 9-18.

- [25] S.V. Gonchenko, On stable periodic motions in systems that are close to systems with a structurally unstable homoclinic curve // *Rus. Math. Notes*, 1980, v.33, 384-389.
- [26] S.V. Gonchenko, L.P. Shilnikov and D.V. Turaev, Homoclinic tangencies of arbitrarily high orders in conservative and dissipative two-dimensional maps, *Nonlinearity*, 2007, **20**, 241-275.
- [27] S.V. Gonchenko, D.V. Turaev and L.P. Shilnikov, Dynamical phenomena in multi-dimensional systems with a non-rough Poincare homoclinic curve // *Russian Acad. Sci. Dokl. Math.*, 1993, v.47, 3, 410-415.
- [28] S.V. Gonchenko, L.P. Shilnikov and D.V. Turaev, On dynamical properties of multi-dimensional diffeomorphisms from Newhouse regions // *Nonlinearity*, 2008, vol. 21, pp. 923–972.
- [29] L. Tedeshini-Lalli and J.A. Yorke, How often do simple dynamical processes have infinitely many coexisting sinks // *Comm. Math. Phys.*, 1995, **106**, pp.635-657.
- [30] S.V. Gonchenko, L.P. Shilnikov and D.V. Turaev, Dynamical phenomena in systems with structurally unstable Poincaré homoclinic orbits // *Chaos*, 1996, v. 6, No.1, 15-31.
- [31] S.V. Gonchenko, Moduli of Ω -conjugacy of two-dimensional diffeomorphisms with a structurally unstable heteroclinic contour // *Sb. Math.* 187, 1261-1281 (1996).
- [32] S.V. Gonchenko, D.V. Turaev and L.P. Shilnikov, Homoclinic tangencies of an arbitrary order in Newhouse domains // *Itogi Nauki Tekh., Ser. Sovrem. Mat. Prilozh.* 67, 69-128 (1999) [English translation in *J. Math. Sci.* 105, 1738-1778 (2001)].
- [33] S.V. Gonchenko, C. Simo and A. Viero, Richness of dynamics and global bifurcations in systems with a homoclinic figure-eight // *Nonlinearity*, 2013, 26(3), 621-678.
- [34] P. Berger, Zoology in the Henon family: twin babies and Milnor’s swallows // *arXiv:1801.05628v1 [math.DS]* 2018.
- [35] S.V. Gonchenko and L.P. Shilnikov, Arithmetic properties of topological invariants of systems with structurally unstable homoclinic trajectories // *Ukr. Math. J.* 39, 15-21 (1987).
- [36] S.V. Gonchenko, Moduli of systems with non-rough homoclinic orbits (the cases of diffeomorphisms and vector fields) // *Methods of the qualitative theory and bifurcation theory*, 34-49 (1989) [English translation in *Sel. Math. Sov.* 11, 393-404 (1992)].

- [37] S.V. Gonchenko and L.P. Shil'nikov, On moduli of systems with a structurally unstable homoclinic Poincaré homoclinic curve // Russian Acad. Sci. Izv. Math., 1993, **41**, No.3, pp. 417-445.
- [38] S.V. Gonchenko and L.P. Shilnikov, Invariants of Ω -conjugacy of diffeomorphisms with a nongeneric homoclinic trajectory // Ukr. Math. J. 42, 134-140 (1990).
- [39] S.V. Gonchenko, Dynamics and moduli of Ω -conjugacy of 4D-diffeomorphisms with a structurally unstable homoclinic orbit to a saddle-focus fixed point // Amer. Math. Soc. Transl., 2000, v.200, No.2, pp.107-134.
- [40] S.V. Gonchenko, Homoclinic tangencies, Ω -moduli and bifurcations // Proc. of the Steklov Inst. of Math., 2002, **236**.
- [41] S.V. Gonchenko and L.P. Shilnikov, On dynamical systems with structurally unstable homoclinic curves // Soviet Math. Dokl., 1986, **33**, No.1, pp.234-238.
- [42] S.V. Gonchenko, D.V. Turaev and L.P. Shilnikov, On models with a non-rough homoclinic Poincaré curve // Methods of qualitative theory and bifurcation theory, Nizhny Novgorod, 36-61 (1991).
- [43] S.V. Gonchenko, O.V. Sten'kin and D.V. Turaev, Complexity of homoclinic bifurcations and Ω -moduli // Int.Journal of Bifurcation and Chaos, v.6, No.6 (1996), pp.969-989.
- [44] S.V. Gonchenko, L.P. Shilnikov, O.V. Sten'kin and D.V. Turaev, Bifurcations of systems with structurally unstable homoclinic orbits and Ω -moduli // Computers Math. Applic., 1997, v. 34, No. 2-4, pp. 111-142.
- [45] S.E. Newhouse, J. Palis and F. Takens, Bifurcations and stability of families of diffeomorphisms // Publ.Math.Inst. Haute Etudes Scientifiques, 1983, **57**, p.5-72.
- [46] M.W. Hirsch, C.C. Pugh and M. Shub, Invariant manifolds // Lecture Notes in Math., vol.583, Springer-Verlag, Berlin, 1977.
- [47] D.V. Turaev, On dimension of non-local bifurcational problems // Int.Journal of Bifurcation and Chaos, 1996, **6**, No.5, pp.919-948.
- [48] J. A. de Oliveira, L. T. Montero, D. R. da Costa, J. A. Mendez-Bermudez, R. O. Medrano, E. D. Leonel, An investigation of the parameter space for a family of dissipative mappings // Chaos 29, 053114 (2019); <https://doi.org/10.1063/1.5048513>
- [49] V.S. Afraimovich, On smooth changes of variables // *Methods of the Qualitative Theory and the Bifurcation Theory*, (E.A.Leontovich-Andronova, ed.), 1984, (Gorky State Univ.), pp.10-21. (Russian).

- [50] L.P. Shilnikov, On a Poincaré-Birkhoff problem // Math. USSR Sb., 1967, **3**, 91-102.
- [51] L.P. Shilnikov, A contribution to the problem of structure of a neighborhood of a homoclinic tube of invariant torus // Soviet Math. Dokl., 1968, **180**, No.2, 286-289. (Russian).
- [52] V.S. Afraimovich, and L.P. Shilnikov, On critical sets of Morse-Smale systems // Trans. Moscow Math. Soc., 1973, **28**.
- [53] I.M. Ovsyannikov and L.P. Shilnikov, On systems with a saddle-focus homoclinic curve // Math. USSR Sbornik, 1987, **58**, 91-102.